

Article

Gene Expression Analysis of Potato (*Solanum tuberosum* L.) Lipoygenase Cascade and Oxylin Signature under Abiotic Stress

Svetlana Gorina *, Anna Ogorodnikova, Lucia Mukhtarova and Yana Toporkova *

Kazan Institute of Biochemistry and Biophysics, FRC Kazan Scientific Center of RAS, P.O. Box 30, 420111 Kazan, Russia; anyuta_ogorodnik@mail.ru (A.O.); lucia74@yandex.ru (L.M.)

* Correspondence: gsvetlana87@gmail.com (S.G.); toporkova@kibb.knc.ru (Y.T.)

Abstract: The metabolism of polyunsaturated fatty acids through the lipoygenase-catalyzed step and subsequent reactions is referred to as the lipoygenase (LOX) pathway. The components of this system, such as jasmonates, are involved in growth, development and defense reactions of plants. In this report, we focus on dynamics of expression of different LOX pathway genes and activities of target enzymes with three abiotic stress factors: darkness, salinity and herbicide toxicity. To obtain a more complete picture, the expression profiles of marker genes for salicylic acid, abscisic acid, ethylene, auxin and gibberellin-dependent signaling systems under the same stresses were also analyzed. The gene expression in *Solanum tuberosum* plants was analyzed using qRT-PCR, and we found that the LOX-cascade-related genes responded to darkness, salinity and herbicide toxicity in different ways. We detected activation of a number of 9-LOX pathway genes; however, in contrast to studies associated with biotic stress (infection), the 9-divinyl ether synthase branch of the LOX cascade was inhibited under all three stresses. GC-MS analysis of the oxylin profiles also showed the main activity of the 9-LOX-cascade-related enzymes after treatment with herbicide and darkness.

Keywords: potato (*Solanum tuberosum* L.); lipoygenase pathway; CYP74 family; abiotic stress



Citation: Gorina, S.; Ogorodnikova, A.; Mukhtarova, L.; Toporkova, Y. Gene Expression Analysis of Potato (*Solanum tuberosum* L.) Lipoygenase Cascade and Oxylin Signature under Abiotic Stress. *Plants* **2022**, *11*, 683. <https://doi.org/10.3390/plants11050683>

Received: 11 January 2022

Accepted: 25 February 2022

Published: 2 March 2022

Publisher's Note: MDPI stays neutral with regard to jurisdictional claims in published maps and institutional affiliations.



Copyright: © 2022 by the authors. Licensee MDPI, Basel, Switzerland. This article is an open access article distributed under the terms and conditions of the Creative Commons Attribution (CC BY) license (<https://creativecommons.org/licenses/by/4.0/>).

1. Introduction

Due to the lack of the capability to move as a means of reacting to changes in their environment, plants have to adapt to environmental stresses in other ways. Oxylin metabolism is one of the plant defense mechanisms. Oxylin are a constantly growing group of low-molecular-weight compounds that comprise oxygenated fatty acids and their derivatives [1]. The main source of oxylin is the lipoygenase (LOX) cascade. The most studied oxylin are jasmonates, products of the allene oxide synthase (AOS) branch of the LOX cascade. Among jasmonates, jasmonoyl-isoleucine (JA-Ile) mediating the plant cell response to biotic and abiotic stresses is the most studied [2]. Besides JA-Ile, the direct effect of a number cyclopentenones (10-oxo-11-phytodienoic acid (10-OPDA), 10-oxo-11-phytoenoic acid (10-OPEA)) on the growth of fungi and herbivorous insects has been described [3,4]. In addition, there is a group of active airborne metabolites such as methyl JA and *cis*-jasmane, which act as messengers between plants to transmit signals and activate defense genes [5]. Other well-studied oxylin are green leaf volatiles (GLVs), composed of C6 aldehydes, alcohols and their esters, formed through the hydroperoxide lyase (HPL) branch of the LOX pathway. These compounds have been shown to play key roles in plant–plant and plant–herbivore interactions [6,7]. Additionally, they function as signals activating systemic defense [8,9], and are involved directly in plant defense as antimicrobials. For example, (2E)-hexenal [10] and (3E)-hexenal [11] possess antibacterial properties, while (2E)-nonenal and (2E)-hexenal exhibit antifungal properties inhibiting hyphal growth [12]. Besides GLVs, the HPL pathway results in formation of traumatic acid, which is involved in wound healing [13].

In addition to AOS and HPL branches, there are divinyl ether synthase (DES) [14–16] and epoxyalcohol synthase (EAS) branches [17] of the LOX pathway. These branches are less studied. The literature describes the participation of divinyl ethers in protection against a number of pathogens: bacteria [18], oomycetes [19] and fungi [20]. The cloning and characteristics of several AOSs, HPLs, DESs and EASs from different plant species revealed that they are closely related members of the cytochrome P450 family, and form the CYP74 family, which is specialized in the metabolism of hydroperoxides [21].

The potato (*Solanum tuberosum* L.) is the most important non-cereal nutritional crop in the world [22], and belongs to the Solanaceae family, which also includes a number of other agricultural crops (tomato, pepper, eggplant), medicinal plants, spices and ornamentals [23]. Potatoes originated in the Andean mountain region of South America, and now there are two main cultivar groups of *Solanum tuberosum*: *andigena* or Andean; and *tuberosum* or Chilean [24]. Cultivated potato species have a base chromosome number of $n = 12$, and can be of different ploidy levels: di-, tri-, tetra- or pentaploid [23].

In this work, we focused on the study of gene expression of the lipoxygenase pathway of potato and other related hormone (auxin, ethylene, abscisic acid, salicylic acid and gibberellin) signaling systems during abiotic stresses. Along with this, the activity of enzymes of the LOX pathway was assessed in the analyzed samples. Our results demonstrate that different types of abiotic stress are characterized by their own pattern of expression of genes of the LOX cascade, as well as by different activities of target enzymes (LOX, CYP74, etc.). Significant changes in oxylipin profiles were associated with the 9-LOX pathway of linoleic acid metabolism. However, in contrast to studies associated with biotic stress (infection), the 9-DES branch of the LOX cascade was inhibited during darkness, salinity and herbicide toxicity.

2. Results and Discussion

2.1. Bioinformatic Analysis of *S. tuberosum* CYP74 Sequences

There are six CYP74 genes in the potato genome, including one DES gene (StDES), one HPL gene (StHPL) and one dual HPL/EAS (StHPL/EAS), as well as three AOS genes (StAOS1, StAOS2 and StAOS3). Based on the NCBI and Phytozome data, the exon–intron structure and localization of potato CYP74 genes was established. AOS genes are localized on the following chromosomes: StAOS1: on the 4 chr; StAOS2: on the 22 chr; and StAOS3: on the 10 chr. The StDES gene is localized on the 1 chr, the StHPL gene is localized on the 7 chr and the StHPL/EAS gene is localized on the 1 chr. AOS genes (StAOS1, StAOS2 and StAOS3) do not have introns; both StHPL and StDES genes have one intron and StHPL/EAS gene has two introns (Figure 1).

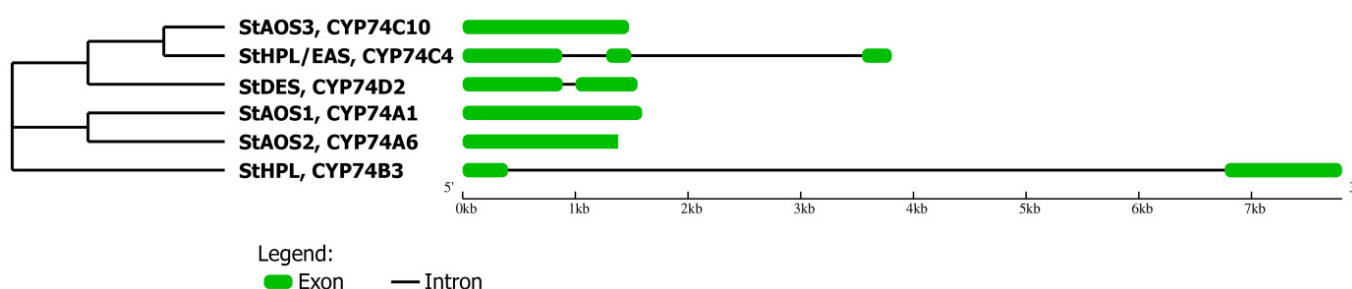


Figure 1. Phylogenetic tree and gene structure of the CYP74 members of *S. tuberosum*. The green areas represent exons; lines show the introns.

The CYP74 enzymes of potato belong to four subfamilies (A, B, C and D), and are classified as follows: CYP74A1 (StAOS1); CYP74A6 (StAOS2); CYP74C10 (StAOS3); CYP74C4 (StHPL/EAS); CYP74B3 (StHPL); and CYP74D2 (StDES). We built a phylogenetic tree to assess the similarity of the CYP74 enzymes (Figure 1). As expected, the CYP74A and CYP74C enzymes group with each other. CYP74D2 is located closer to the CYP74C members, while CYP74B3 is located separately from other enzymes.

2.2. Cis-Element Analysis of *S. tuberosum* CYP74 Genes

To assess the possible transcriptional regulation of potato CYP74 genes, 1000 bp sequences upstream of the translation start site were scanned by PlantCARE and PLACE. Various regulatory elements were found in the promoter regions of the CYP74 genes, among which the widely represented were the following elements: involved in light responsiveness (such as Box 4, G-Box, GT1-motif, TCT-motif, MRE, I box, SORLIP1AT), involved in the abscisic acid responsiveness (ABRE), required for etiolation-induced expression (ACGTATERD1, ABRELATERD1) and playing a role in responses to pathogens and salinization (GT1GMSCAM4) (Figure 2). One to six (depending on the gene) salicylate-responsive elements (TCA-element, WBOXATNPR1), auxin-responsive elements (TGA-element, NTBBF1ARROLB, gibberellin-responsive elements (MYB, P-box, GARE1OSREP1) and transcriptional repressor of the gibberellin pathway (WRKY71OS) (Figure 2) were also detected. *Cis*-elements, their sequences and the corresponding database are shown in Table 1. Thus, the analysis of regulatory elements carried out showed that the promoter regions of genes containing *cis*-acting elements responded to abiotic stresses, light and phytohormones, etc.

Table 1. *Cis*-elements detected in 1 kbp upstream region of CYP74 genes of *S. tuberosum*: MRE: MYB-recognition element; SORLIP1AT: sequences over-represented in light-induced promoters; ABRE: abscisic acid responsiveness; ACGTATERD1: ACGT sequence required for etiolation-induced expression of *erd1* (early responsive to dehydration); ABRELATERD1: ABRE-like sequence required for etiolation-induced expression of *erd1*; WBOXATNPR1: W-box found in promoter of Arabidopsis NPR1 gene; GT1GMSCAM4: GT-1 motif found in the promoter of soybean (*Glycine max*) CaM isoform, SCaM-4; GARE1OSREP1: gibberellin-responsive element (GARE) found in the promoter region of a cysteine proteinase (REP-1) gene in rice.

Functions of <i>cis</i> -Elements	<i>Cis</i> -Element	Sequence	Tools Used
Light responsiveness	Box 4	ATTAAT	PlantCARE
	G-Box	CACGTC, CACGTT, TACGTG	PlantCARE
	GT1-motif	GGTTAA	PlantCARE
	TCT-motif	TCTTAC	PlantCARE
	MRE	AACCTAA	PlantCARE
	I box, SORLIP1AT	GCCAC	PLACE
Abscisic acid	ABRE	ACGTG, CACGTG, CACGTA	PlantCARE
Etiolation-induced	ACGTATERD1	ACGT	PLACE
	ABRELATERD1	ACGTG	PLACE
Pathogen and salt-induced	GT1GMSCAM4	GAAAAA	PLACE
Salicylic acid	TCA-element	CCATCTTTT	PlantCARE
	WBOXATNPR1	TTGAC	PLACE
Auxin-responsive element	TGA-element	AACGAC	PlantCARE
	NTBBF1ARROLB	ACTTTA	PLACE
Gibberellin-responsive	MYB	CAACCA, TAACCA	PlantCARE
	P-box	CCTTTTG	PlantCARE
	GARE1OSREP1	TAACAGA	PLACE
Repressor of the gibberellin pathway	WRKY71OS	TGAC	PLACE

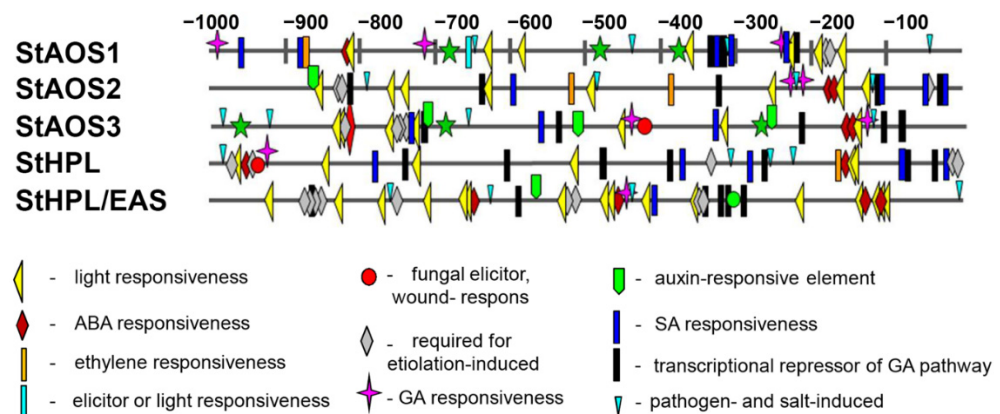


Figure 2. Distribution of *cis*-elements identified in *S. tuberosum* CYP74 genes. Different colors and shapes represented different *cis*-acting elements, which are most enriched in the promoter regions up to -1000 from CYP74 genes.

2.3. Expression Analysis of Marker Genes of Lipoxygenase Cascade and Other Signaling Systems of *S. tuberosum* after Growing in the Dark

To investigate the dynamics of expression pattern of genes of lipoxygenase cascade (Supplementary Table S1) in potato plants in conditions of darkness, salinity and herbicide toxicity, we monitored mRNA levels in shoots and roots in different time intervals after treatments by qRT-PCR. Etiolation involves prolonged growth in the absence of light, resulting in the formation of etioplasts, structures which do not contain chlorophyll or stacked thylakoid membranes, and the lipid composition of which consists mainly of monogalactosyldiacylglycerol (MGDG) and digalactosyldiacylglycerol (DGDG) [25,26]. Additionally, as was shown earlier in Arabidopsis [27], during etiolation, the content of unsaturated C18 fatty acids (oleic (18:1), linoleic (18:2) and α -linolenic (18:3) acids) in cutin polymer of etiolated hypocotyls increases. In higher plants, the main substrates of the lipoxygenase cascade are linoleic and α -linolenic acids.

Darkness of potato plants led to a gradual pronounced decrease in *StHPL* expression by two orders of magnitude in shoots and by one order of magnitude in roots compared to the control (Figure 3). Expression of *StDES* had a similar pattern. The expression of *StHPL/EAS* slightly (2–4 times) increased in shoots, and remained at the control level in roots. *StAOS3* expression gradually increased, and in 7 days it differed by 10 times from the control, both in shoots and roots. Expression pattern of *StAOS1* and *StAOS2* were opposite: expression of *StAOS1* slightly increased in shoots and decreased in roots, while expression of *StAOS2* decreased in shoots and increased in roots. Apparently, a switch between two AOS branches occurred. Along with this, *StLOX* expression increased only in roots, while in shoots it remained comparable with control values. It is interesting that the most pronounced increase in shoots was observed for allene oxide cyclase (*StAOC*) by almost three orders of magnitude in all analyzed samples. In roots, *StAOC* expression also increased. It was previously shown that an increase in the AOC gene expression level can be induced by wounding [28]; however, the accumulation of AOC mRNA may not lead to the accumulation of jasmonates [29,30], and as a consequence, the appearance of a JA response. Apparently, along with the regulation of JA signaling at the level of signal transduction, there is a regulation mechanism through a limiting substrate. This mechanism activates expression of upstream genes of the JA biosynthetic pathway, such as AOC, to provide a sufficient amount of substrate for a quick response if needed. The greatest increase in AOC expression in shoots is consistent with the previously established existence of JA transport (or its precursors) from shoots to roots [31].

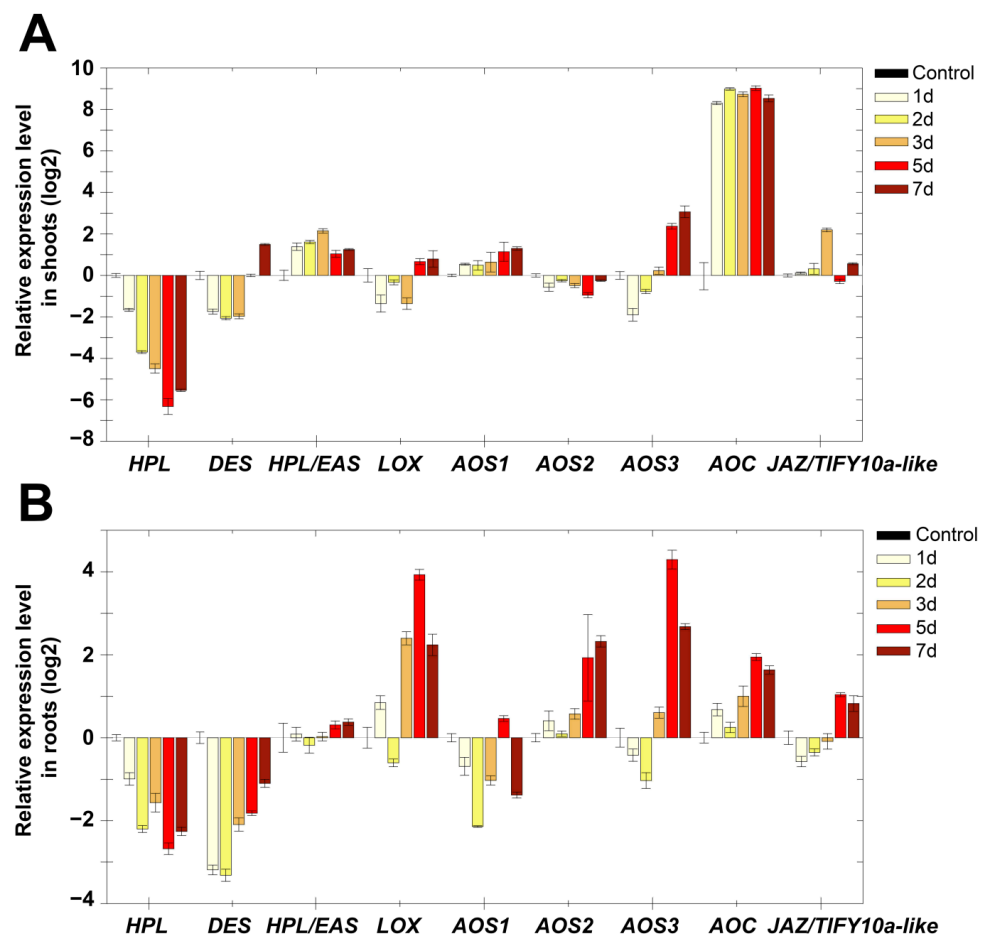


Figure 3. Dynamics of lipoxigenase cascade gene expression (log2) during darkness in shoots (A) and roots (B) in 1, 2, 3, 5 and 7 days. Abbreviations: HPL: hydroperoxide lyase, DES: divinyl ether synthase, HPL/EAS: hydroperoxide lyase/epoxyalcohol synthase, LOX: lipoxigenase, AOS: allene oxide synthase, AOC: allene oxide cyclase and JAZ/TIFY10a-like: JAZ/TIFY transcription regulator gene.

The expression of the allene oxide cyclase (StAOC) encoding gene is greatly increased in the absence of AOS gene expression activation, and requires separate consideration. Apparently, the cyclase reaction in this case is limiting in the biosynthesis of jasmonic acid, while AOS forms a large amount of allene oxide regardless of the presence or absence of stress. However, since allene oxide is a short-lived product that cannot be deposited, in the absence of stress (in the absence of a sufficient amount of cyclase), all excess allene oxide is hydrolyzed to α -ketol.

Apparently, one can observe switching from the HPL and DES branches of lipoxigenase cascade to AOS ones, wherein AOSs are participants of different branches producing different compounds. StAOS1 and StAOS2 catalyze the formation of allene oxide 12,13-EOT ((9Z,11E,13S,15Z)-12,13-epoxy-(9,11,15)-octadecatrienoic acid), a precursor of jasmonic acid, while StAOS3 is a participant in 9-lipoxigenase branch products, which include ketols and cyclopentenones. Patterns of expression of AOS genes indicate that in the shoots, the jasmonate pathway (13-LOX branch) is activated, while in roots, both 9-LOX and 13-LOX pathways are activated.

Since in plant cells, crosstalk between lipoxigenase cascade and other signaling pathways (auxin (indole-3-acetic acid, IAA), gibberellin (GA), ethylene (ET), abscisic acid (ABA) and salicylic acid (SA)) occurs [32–36], the expression of a number of marker genes (Supplementary Table S2) of other signaling pathways was analyzed under the same conditions. Analysis of the expression of marker genes for 7 days during darkness showed that the pattern of gene expression was comparable in shoots and roots (Figure 4). It

was shown that darkness led to a slight accumulation of transcripts of the isochorismate synthase (ICS) gene, which is involved in the biosynthesis of salicylic acid. The level of transcripts of this gene was increased compared to the control in shoots up to 2.6 times, and in roots up to 2.8 times. The incubation of plants in the dark induced a gradual accumulation of most ABA marker genes both in shoots and roots. The following changes were observed in roots: 9-*cis*-epoxycarotenoid dioxygenase (NCED, ABA biosynthesis) (from 0 to 72 times), ABA-8'-hydroxylases (CYP707A, ABA degradation) (from 0 to 666 times), serine/threonine phosphatase 2C (PP2C, negative regulator of ABA signal transmission) (from 0 to 13 times), as well as another important participant in ABA signaling, a transcription factor ABF2 belonging to the ABRE-binding bZIP proteins designated as ABF family (from 0 to 20 times). The shoots had the same pattern, but with slightly less pronounced dynamics. In contrast to those described above, only the lipid transfer ABA-dependent protein (LTP) coding gene was characterized by a lower level of expression up to 0.5-fold in shoots, and a gradual increase from 0.3- to 5-fold compared to the control.

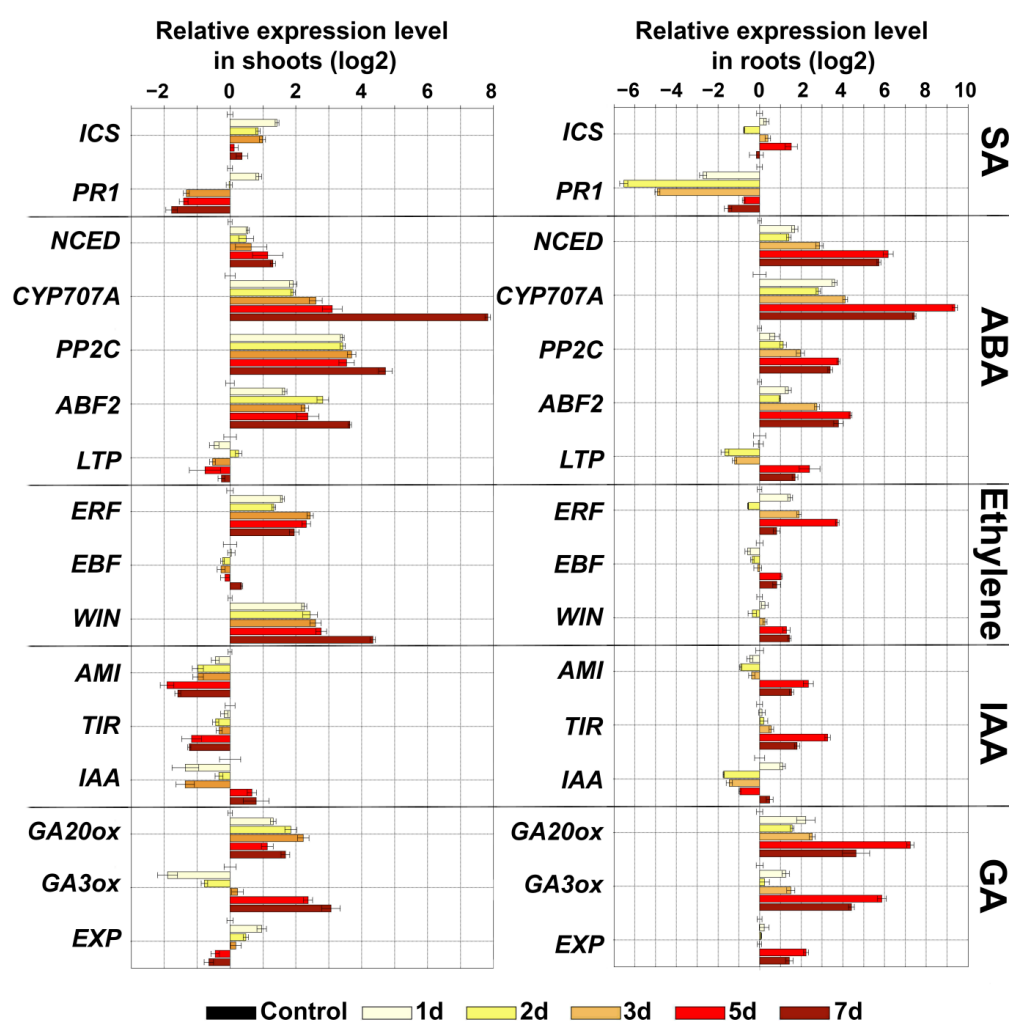


Figure 4. Changes of expression of marker genes of different signaling pathways during darkness in shoots and roots in 1, 2, 3, 5 and 7 days. Abbreviations: ICS: isochorismate synthase, PR1: pathogenesis-related protein 1, ERF: ethylene-inducible transcription factor, EBF: EIN3 (ETHYLENE-INSENSITIVE3) BINDING F-BOX1, WIN: wound-induced (WIN) protein, NCED: 9-*cis*-epoxycarotenoid dioxygenase, CYP707A: ABA-8'-hydroxylases, ABF2: ABRE-binding bZIP proteins, PP2C: serine/threonine phosphatase 2C, LTP: lipid transfer protein, GA20ox: gibberellin (GA) 20-oxidase, GA3ox: GA3 oxidase, EXP: expansins, AMI: indole-3-acetamide hydrolase, TIR: transport inhibitor response and IAA: indole-3-acetic acid inducible 28 (IAA28).

One of the defense mechanisms is associated with ethylene, since expression of genes of ethylene-inducible transcription factor (ERF) and a wound-induced (Win) protein, which also has an ethylene-dependent character of transcription [37], increased. Expression of the gene of the negative regulator of ethylene-dependent signaling *EBF* (EIN3 (ETHYLENE-INSENSITIVE3) BINDING F-BOX1) remained comparable to the control. Growth of plants in the dark, as expected, led to an increase in the expression of genes encoding enzymes of gibberellin biosynthesis (GA3 oxidase (GA3ox), GA20-oxidases (GA20ox)). The darkness did not significantly affect the expression of the *EXP* gene. The level of transcripts of this gene gradually decreased in shoots from 1.9 to 0.6 times, and increased from 1 to 4 times in roots compared to the control. Additionally, the expression level of indole-3-acetamide hydrolase (*AMI*, auxin biosynthesis) and transport inhibitor response (*TIR1*) genes in shoots gradually decreased from 0.7 to 0.25 and from 0.9 to 0.4, respectively. The expression level of the repressor of IAA signaling (*IAA28*) gene gradually increased from 0.3 to 1.7 times. In the roots, the expression pattern was reversed. The level of transcripts increased from 0.71 to 5 and from 1 to 9 for *AMI* and *TIR1*, respectively. The expression level of *IAA28* decreased to 0.3.

Thus, growing potato plants in the dark is associated with the activation of the biosynthesis of jasmonates and gibberellins, as well as the biosynthesis and active utilization of ABA. The presence of ABA in cells is indirectly evidenced by the accumulation of transcripts of *PP2C* and *ABF2* genes, which are both ABA-inducible. These results are consistent with the data on the effect of ABA promotion on the growth of etiolated tomato seedlings [38]. The function of ABA is dose-dependent, and ranges from stimulatory to inhibitory effects [39]. Thus, the accumulation of *PP2C* gene transcripts indicates a fine-tuned regulation of the ABA content.

The absence of light also led to the accumulation of gibberellins [40], which in this study is evidenced by the accumulation of transcripts of *GA3ox* and *GA20ox* genes of gibberellin biosynthesis. Additionally, the relationship between not only ABA and GA but also GA and JA was established. Moreover, these relationships exhibited both antagonistic and synergistic interactions [41–43]. Thus, a significant accumulation of *GA20ox* and *GA3ox* transcripts (by one to two orders of magnitude relative to the control), along with the predominance of gene expression of the 9-LOX pathway over the 13-LOX pathway (Figure 3), testifies to the GA response and inhibition of JA. Changing patterns of gene expression indicate complex cross-signaling required for the adaptation and growth of plants in darkness.

2.4. Expression Analysis of Marker Genes of Lipoxygenase Cascade and Other Signaling Systems of *S. tuberosum* during Oxidative Stress

To investigate the role of lipoxygenase cascade enzymes during oxidative stress, reactive oxygen species (ROS) generation was induced by the addition of 10^{-5} and 10^{-6} M paraquat. Paraquat is one of the most widely used non-selective herbicides. It is a potent inducer of oxidative stress, leading to an increase in ROS production, as well as suppressing the regeneration of reducing equivalents and compounds required for the antioxidant system [44].

The results showed that treatments with paraquat in both concentrations (10^{-5} and 10^{-6} M) in shoots and roots did not affect or lead to a decrease in the expression level of most genes of the lipoxygenase cascade Figure 5. The exception was the *JAZ/TIFY* transcription regulator gene (*JAZ/TIFY10a-like*), the expression of which increased in roots by an order of magnitude at both concentrations of paraquat compared to the control. In literature, this class of regulators is described as negative regulators of jasmonate signaling that repress transcription factors such as *MYC2* [45,46]. However, their expression increases upon the infection of plants [47], which is associated with the strong activation of the jasmonate response and the subsequent activation of the *JAZ/TIFY* genes. It was shown that abiotic stress also affects the increase in *JAZ/TIFY* expression [48], including the studied *TIFY10a* [49]. Thus, the transgenic *Medicago sativa* plants overexpressing *GsTIFY10a* (*Glycine soja*) gene grows better under alkaline stress [49], since overexpression of *GsTIFY10a*

promoted an increase in the expression of genes necessary for maintaining homeostasis, cytoplasmic pH regulation and osmotic regulation (*NADP-ME*, *H⁺-ppase*, *P5CS*) [49,50]. In the present work, an increase in the expression of *JAZ/TIFY10a-like* may indicate both a general response to abiotic stress and suppression of the jasmonate response, since other genes of jasmonate biosynthesis are also down-regulated.

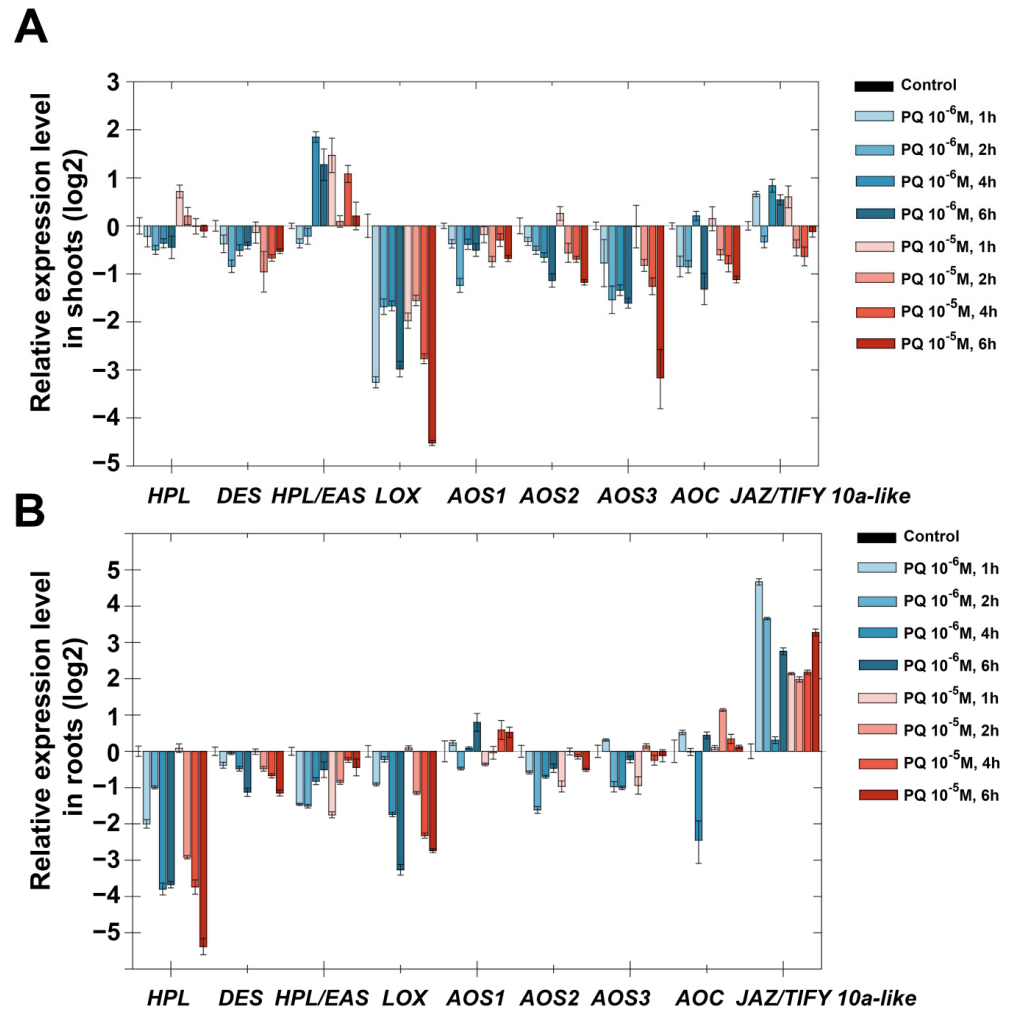


Figure 5. Dynamics of lipoxigenase cascade gene expression after treatment with paraquat (PQ) (10^{-5} (red) and 10^{-6} (blue) M) in shoots (A) and roots (B) in 1, 2, 4 and 6 h. Abbreviations: HPL: hydroperoxide lyase, DES: divinyl ether synthase, HPL/EAS: hydroperoxide lyase/epoxyalcohol synthase, LOX: lipoxigenase, AOS: allene oxide synthase, AOC: allene oxide cyclase and JAZ/TIFY10a-like: JAZ/TIFY transcription regulator gene.

The expression pattern of marker genes after treatment with paraquat (Figure 6) was different from that during darkness. In shoots and roots, the number of ICS gene transcripts was reduced in all samples. In roots, the NCED gene transcripts gradually accumulated in 6 h after treatment (up to 4 times), followed by the accumulation of the PP2C gene transcripts (up to 2 times), while the LTP gene expression decreased (from 8 times in 1 h to values below the control by 6 h). Expression of two other marker genes of ABA signaling (*CYP707A* and *ABF2*) decreased in roots in all experimental samples. In shoots, the expression of almost all ABA marker genes was lower than in the control. Thus, the expression of the NCED gene in the first hour after treatment was lower than in the control by an order of magnitude, and only in 6 h after treatment reached the level of control value. The expression of PP2C, *ABF2* and *LTP* genes was stably lower than in the control, and *CYP707A* gene expression was comparable to the control.

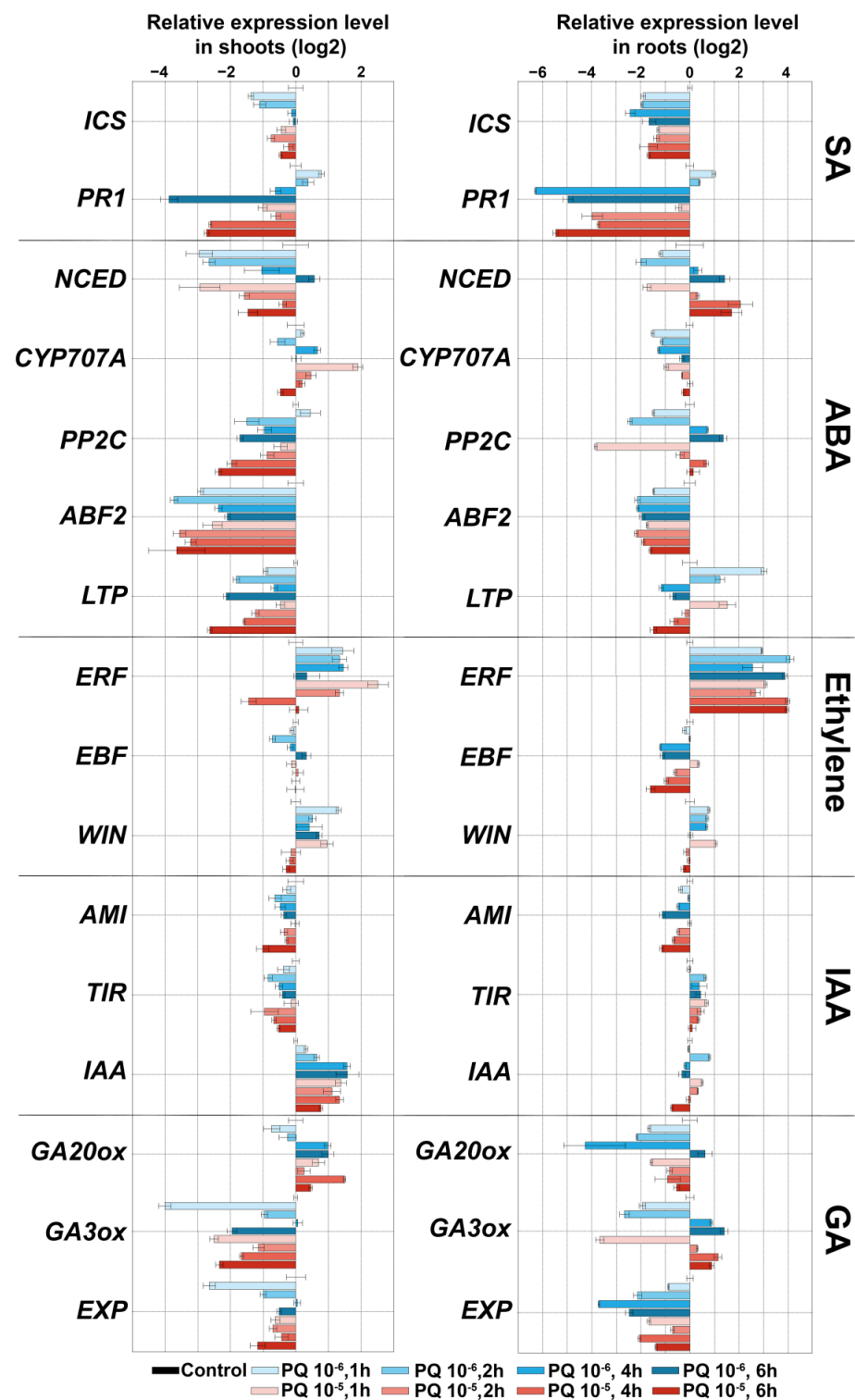


Figure 6. Changes in marker gene expression of other signaling pathways after treatment with paraquat (PQ) (10^{-5} M (red) and 10^{-6} M (blue)) in shoots and roots in 1, 2, 4 and 6 h. Abbreviations: ICS: isochorismate synthase, PR1: pathogenesis-related protein 1, ERF: ethylene-inducible transcription factor, EBF: EIN3 (ETHYLENE-INSENSITIVE3) BINDING F-BOX1, WIN: wound-induced (WIN) protein, NCED: 9-*cis*-epoxycarotenoid dioxygenase, CYP707A: ABA-8'-hydroxylases, ABF2: ABRE-binding bZIP proteins, PP2C: serine/threonine phosphatase 2C, LTP: lipid transfer protein, GA20ox: gibberellin (GA) 20-oxidase, GA3ox: GA3 oxidase, EXP: expansins, AMI: indole-3-acetamide hydrolase, TIR: transport inhibitor response and IAA: indole-3-acetic acid inducible 28 (IAA28).

The expression pattern of ethylene marker genes after the treatment of paraquat was similar to that during darkness: *ERF* and *WIN* expression increased and *EBF* expression was comparable to the control in shoots, and decreased in the roots up to 0.3 times. Expression of *AMI* and *TIR1* genes decreased in shoots up to 0.4 and 0.5 times, respectively, while *IAA28* gene expression slightly increased up to 2.5 times. In the roots, the number of transcripts of *AMI* was also reduced by 0.4 times, while *TIR1* increased to 1.5 times and *IAA28* decreased from 1.7 to 0.5 times. The expression of genes of GA biosynthesis, in contrast to the darkness, did not have a definite pattern, and fluctuated depending on the experimental point. In the shoots, the expression of the *GA20ox* gene increased from 0.6 to 2 times, while the expression of the *GA3ox* gene decreased up to 0.06 times (at PQ 10^{-6} M) and up to 0.15 times (at PQ 10^{-5} M). In the roots, on the contrary, the expression of *GA20ox* gene decreased (up to 0.2 times), while the *GA3ox* gene expression had a slight upward trend (up to 2.5 times) in 14 days. The *EXP* gene expression was reduced in all samples compared to the control plants.

ABA is one of the main phytohormones involved in defense responses to drought, salt, osmotic or cold stress [51,52]. Paraquat treatment also led to changes in the expression of ABA marker genes (*NCED*, *CYP707A*, *PP2C*, *ABF2* and *LTP*) (Figure 6). In the roots, there was a slight activation of the ABA biosynthesis gene (*NCED*) from 0.4 to 4.5 times. The number of *NCED* transcripts in the shoots was reduced by an order of magnitude (up to 0.1 times). The expression of genes with an ABA-dependent expression pattern in shoots was also reduced, from *PP2C* to 0.2, *ABF2* to 0.07 and *LTP* to 0.15 times, respectively. Along with this, activation of transcription of the *CYP707A* gene was observed (up to 3 times, degradation of ABA). In the roots, along with a decrease in the expression of the *ABF2* gene (up to 0.2 times), the number of transcripts of the *PP2C* gene gradually increased from 0.3 to 2.5, while the number of the *LTP* gene, on the contrary, decreased from 8 to 0.3 times. The results obtained, along with the activation of ABA biosynthesis genes, indicated a possible inhibition of ABA signal transduction. The picture of ABA signaling in shoots and roots most likely differed, since the patterns of gene expression did not match.

A clearer picture was observed for ethylene. An increase in the expression of *ERF* and *WIN* (in shoots and roots) indicated the activation of ethylene-dependent genes, which is consistent with the data that ET signaling and biosynthesis are induced under various agents causing oxidative stress [53]. In this case, the expression of *ERF* genes is important for signaling and expression of genes of the antioxidant system [54,55]. The expression of auxin-related and GA-related genes was comparable to the control. As a whole, ET signaling was activated and SA and JA signaling inhibited. GA and auxin signaling did not differ from control.

2.5. Expression Analysis of Marker Genes of Lipoxygenase Cascade and other Signaling Systems of *S. tuberosum* after Treatment with NaCl

Salt stress not only has a negative effect on biochemical processes in plants, but also reduces their agricultural value. Moreover, the salinity toxicity problems are gradually increasing around the world [56]. In this regard, the present work on study the effect of NaCl-induced salt stress on expression of marker genes of lipoxygenase cascade and other signaling systems is of current interest. The results showed that the expression profile of target genes in shoots and roots had differences.

Treatment with NaCl (25, 50 and 100 mM) led to a decrease in the expression of *StDES*, *StHPL/EAS*, *StAOS2* and *StAOS3* in shoots throughout all time points (Figure 7A). The expression of *StAOS1*, *StHPL*, *StAOC* and *StJAZ/TIFY10a-like* was comparable to the control or slightly reduced. In roots, genes of the lipoxygenase cascade had similar expression patterns under treatment with NaCl (Figure 7B). The expression of *StAOS3* and *StHPL* noticeably increased, and the expression of *StAOS3* was maximal on the first day (100 times more than in the control sample), and displayed a declining trend for 14 days, while the expression pattern of *StHPL* was reversed—the maximal accumulation of transcripts was observed in 14 days. Other lipoxygenase cascade genes possessed smaller changes of expression dynamics in comparison with *StAOS3* and *StHPL*. The expression of *StHPL/EAS*,

StAOC and *StLOX* was comparable to the control; the expression of *StDES*, *StAOS1*, *StAOS2* and *StJAZ/TIFY10a-like* tended to gradually decrease in 14 days.

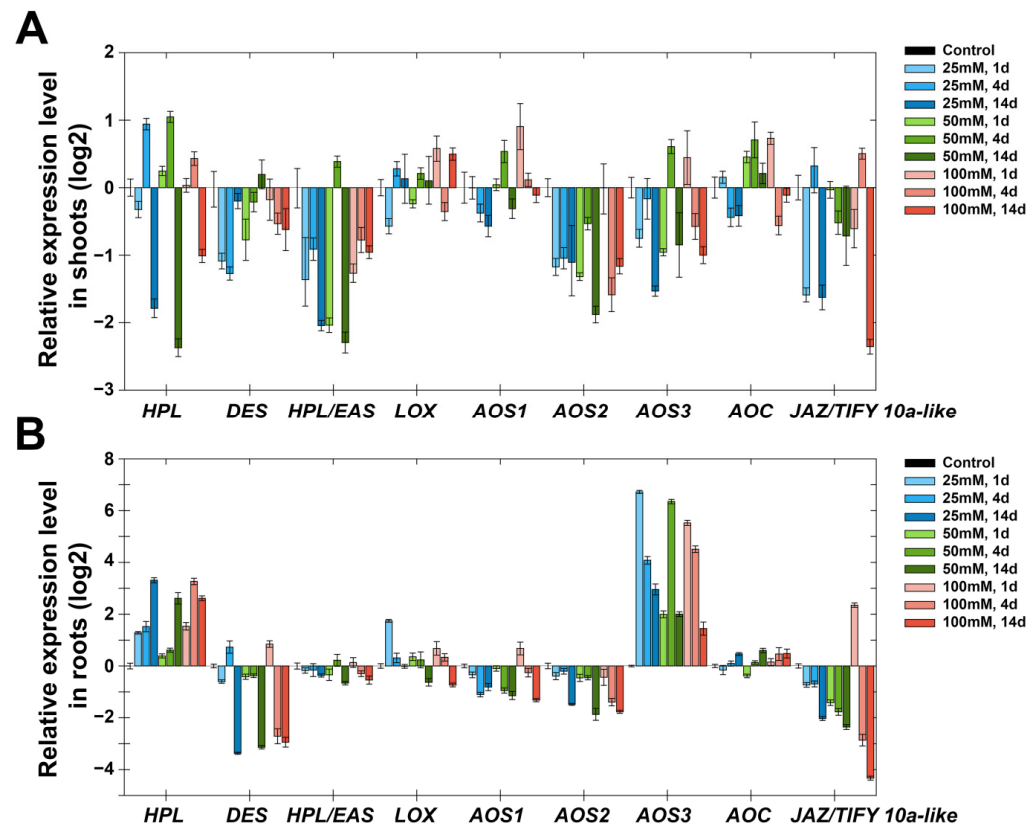


Figure 7. Expression of lipoxigenase cascade genes in response to treatment with NaCl (25, 50, 100 mM) in shoots (A) and roots (B). The blue color indicates the concentration of 25, while green denotes 50 and red 100 mM. The color gradation indicates samples at 1, 4 and 14 days. Abbreviations: HPL: hydroperoxide lyase, DES: divinyl ether synthase, HPL/EAS: hydroperoxide lyase/epoxyalcohol synthase, LOX: lipoxigenase, AOS: allene oxide synthase, AOC: allene oxide cyclase and JAZ/TIFY10a-like: JAZ/TIFY transcription regulator gene.

An increase in *StAOS3* expression in roots rather than in shoots is in good agreement with the subcellular localization of this enzyme. On the basis of immunolocalization, it was shown that the specific signal was detected at amyloplasts and leucoplasts from the subterranean organs, but not at mesophyll chloroplasts [57], in contrast to other CYP74 enzymes (*StAOS1*, *StAOS2* and *StHPL*) localized in chloroplasts [58]. In green parts, *StAOS3* was found only in a subset of plastids, specifically amyloplasts and non-differentiated plastids in the stelar parenchyma [57]. Thus, in roots under salt stress, the biosynthesis of 9-AOS products by *StAOS3* is activated. An increase in the expression of *StAOS3* in shoots during darkness (Figure 3) may indicate that the above-ground and underground parts become similar in a number of signs. The suppression of the expression of the negative regulator JAZ/TIFY of jasmonate signal transmission [45,46] is in good agreement with the data on the role of jasmonates in salt stress [59,60], since when the negative regulator is removed, the transcription of JA-induced genes is activated [61]. In addition, experimental data show that salt-tolerant varieties of tomatoes (close relatives of potatoes) have higher levels of jasmonates than salt-sensitive varieties [62].

NaCl treatment caused a small accumulation of transcripts of the ICS gene (SA biosynthesis) in shoots (1.5–7 times) and roots (2–6 times), while significant changes in expression of marker genes of ABA signaling were observed only in roots (Figure 8). Gradually in 14 days after treatment with 25 and 50 mM NaCl and on the first day after treatment with 100 mM NaCl, the expression of *NCED* gene (ABA biosynthesis) was induced by up to

10 times more in comparison to the control. However, there was also a gradual accumulation of the CYP707A gene transcripts (ABA degradation) in 14 days after treatment with 25 and 50 mM (up to 80 and 40 times, respectively). Moreover, the expression of the CYP707A gene was maximal already on the first day after treatment with 100 mM NaCl. Additionally, the transcription of the PP2C gene (negative regulator of ABA signal transmission) and ABF2 transcription factor was slightly activated. Expression of the LTP gene (with an ABA-dependent expression pattern) decreased by an order of magnitude.

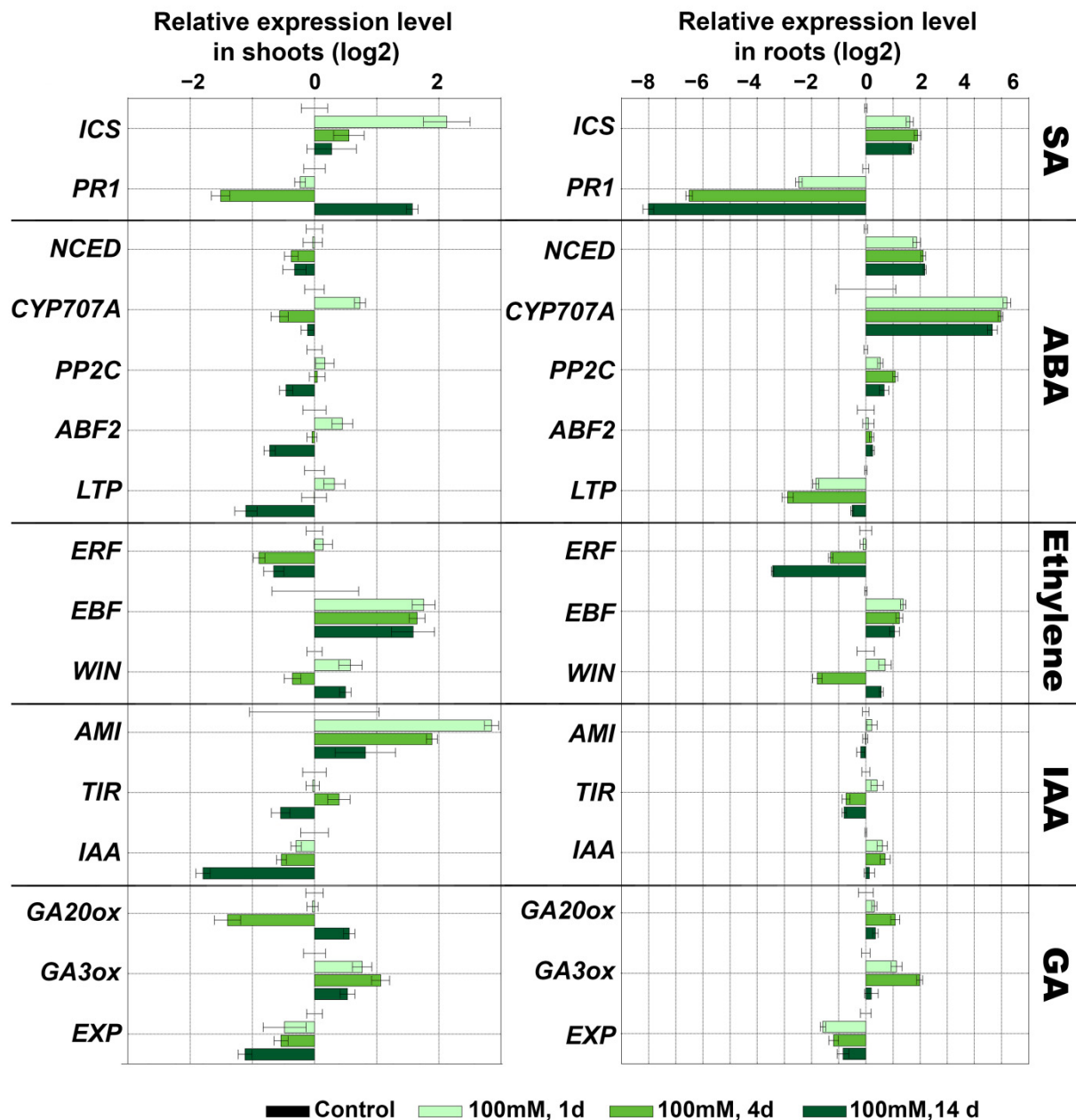


Figure 8. Changes in marker gene expression of other signaling pathways in response to treatment with NaCl (100 mM) in shoots and roots. Abbreviations: ICS: isochorismate synthase, PR1: pathogenesis-related protein 1, ERF: ethylene-inducible transcription factor, EBF: EIN3 (ETHYLENE-INSENSITIVE3) BINDING F-BOX1, WIN: wound-induced (WIN) protein, NCED: 9-*cis*-epoxycarotenoid dioxygenase, CYP707A: ABA-8'-hydroxylases, ABF2: ABRE-binding bZIP proteins, PP2C: serine/threonine phosphatase 2C, LTP: lipid transfer protein, GA20ox: gibberellin (GA) 20-oxidase, GA3ox: GA3 oxidase, EXP: expansins, AMI: indole-3-acetamide hydrolase, TIR: transport inhibitor response and IAA: indole-3-acetic acid inducible 28 (IAA28).

Salt treatment induced a gradual decrease in transcription of the ERF gene (ethylene-dependent gene) (from 1 to 0.5 in shoots and from 0.9 to 0.09 in roots) and an increase in transcription of the EBF gene (negative regulation of ethylene signaling) (up to 4 times in shoots; up to 3 times in roots). Additionally, in roots, a decrease in the expression of the WIN gene (up to 2 times) was observed. In shoots, expression of this gene was comparable to the control. The data indicated a possible inhibition of ethylene signaling. In shoots, the expression of the AMI gene (auxin biosynthesis) increased by 2–14 times, while the expression of the IAA28 gene (repressor of IAA signaling) decreased by 2–8 times (Figure 8). Expression of the TIR1 gene slightly differed from the control values depending on the experimental point. In roots, the pattern of expression of these genes was opposite, but not significantly. The expression of genes of GA biosynthesis differed depending on the experimental point and had no clear picture. In the leaves at all three NaCl concentrations, at most points, the expression of the GA20ox gene decreased to 0.3, while the expression of the GA3ox gene increased to 2 (Figure 8 and Supplementary Figure S1). In the roots, on the contrary, at all three NaCl concentrations, at most points, an increase in the expression of the GA20ox gene to a value of 2 was observed. The expression of the GA3ox gene after treatment with 25 and 50 mM NaCl decreased to a value of 0.2 (Supplementary Figure S1), while after treatment with 100 mM NaCl it increased by 4 times.

Since the main organs of GA biosynthesis are considered to be young leaves and the expression of GA biosynthesis genes in the shoots was reduced in most samples (excluding GA3ox after treatment with 100 mM NaCl), this may indicate the inhibition of the GA pathway.

An increase in the expression of the ICS gene indicates its participation in adaptive regulation during salinity, and is consistent with previous studies [63,64]. As shown earlier, SA enhances the antioxidant system and the synthesis of osmolytes, and promotes plant photosynthesis under salt stress [65]. An increase in the expression of the NCED gene (ABA biosynthesis) is consistent with the literature data on the role of ABA as one of the key hormones in plant adaptation to salt stress [66,67]. Along with the activation of ABA biosynthesis, there is activation of auxin biosynthesis (in shoots), which plays an important role in the formation of lateral roots. High NaCl concentrations inhibit the development of lateral roots through ABA-coordinated polar auxin transport [68–70]. Apparently, the ABA-8'-hydroxylase gene is activated to regulate the level of ABA. This is necessary for functioning of the auxin system, as auxin transport is ABA-dose-dependent. The inhibition of the expression of genes of GA biosynthesis may be explained by switching to other signaling pathways. Additionally, regulating GA levels may be a mechanism of plant adaptation to growth inhibition due to salt stress. It corrects the growth rate in accordance with changing environmental conditions. Thus, genes associated with GA catabolism in *Arabidopsis* (*AtGA2ox7* [71]) and rice (*OsGA2ox5* [72]) increase plant resistance to salt by slowing growth. Along with the central players, ABA, GA and auxins participating in the regulation of adaptation and growth under salt stress, new players become involved, including enzymes of the lipoxygenase cascade (Figure 7). Thus, salt stress, being multifaceted and multicomponent, causes a significant response in signaling systems, provoking the solution of various tasks.

2.6. Activity of Lipoxygenase Cascade-Related Enzymes after Treatment with NaCl, Paraquat and Darkness

The activity of the target enzymes of the lipoxygenase cascade (LOX, CYP74s, etc.) in shoots and roots was analyzed as a result of accumulation of the corresponding oxylipins in plant extracts after incubation with linoleic and alpha-linolenic acids. Oxylipin composition is considered to reflect the physiological/functional state of a plant; therefore, the term 'oxylipin signature' has been put forward [73]. The internal standard was margaric acid (17:0), which is not converted during the lipoxygenase cascade. The following samples were analyzed by GC-MS: 1 day after treatment with 100 mM NaCl; 5 days after moving plants

into the dark; and 4 h after treatment with 10^{-6} mM paraquat. These samples possessed the maximal expression of lipoxygenase cascade genes.

In control shoots and roots, the transformation of linoleic and α -linolenic acids by lipoxygenases into the corresponding hydroperoxides, which further serve as substrates for the CYP74 enzymes, was observed. In shoots and roots, the main product of lipoxygenase conversion was linoleic acid 9-hydroperoxide (compound **1**). Moreover, its content in the shoots (Figure 9A) was twice as high as in the roots (Figure 10A). 9-Hydroperoxide of α -linolenic acid (compound **2**), as well as 13-hydroperoxides of linoleic and α -linolenic acid (compound **3**), were detected in a significantly smaller quantity. Their content in the leaves was three times higher than in the roots. Additionally, the roots contained a significant number of 9-AOS pathway products, as evidenced by the appearance of the corresponding peaks **5a/5b** and **6a/6b** in the chromatogram. Compounds **5a** and **5b** had the same mass spectral patterns, which are depicted in Supplementary Figure S2 and possessed M^+ at m/z 472 (0.1%), $[M-Me]^+$ at m/z 457 (0.5%), $[M-MeO]^+$ at m/z 441 (2%), $[M-C11/C18]^+$ at m/z 361 (11%), $[M-C10/C18 + TMS]^+$ at m/z 332 (3%), $[361-TMSOH]^+$ at m/z 271 (58%), $[M-C10/C18]^+$ at m/z 259 (56%), $[M-C1/C9]^+$ at m/z 213 (31%), m/z 155 (58%), m/z 129 (32%), m/z 109 (25%) $[CH_2 = O^+ - SiMe_3]$ at m/z 103 (31%) and $[SiMe_3]^+$ m/z 73 (100%). The spectrum matched that of the product of $NaBH_4$ reduction in the α -ketol, 9-hydroxy-10-oxo-12-octadecenoic acid (Me/TMS). Compounds **6a** and **6b** also possessed the identical mass spectra, which are depicted in Supplementary Figure S3. Mass spectra were similar to those of compounds **5a** and **5b** and corresponded to the product of $NaBH_4$ reduction in the α -ketol, 9-hydroxy-10-oxo-12,15-octadecadienoic acid (Me/TMS). α -Ketols synthesized from 9-HPOD (**5a** and **5b**) and 9-HPOT (**6a** and **6b**) were present in equal quantities. Additionally, the control roots contained 9-oxononanoic acid (9-HPL product), while the control shoots did not. The products of the 9-EAS pathway, 9,10-epoxy-11-hydroxy-12-octadecenoic acid (compound **4**), were also found.

Analysis of GC-MS chromatograms showed that darkness led to the accumulation of all linoleate and linolenate hydroperoxides (9-HPOD, 9-HPOT, 13-HPOD and 13-HPOT) in roots (especially 9-HPOD). These data are consistent with the results on the expression of the *StLOX* gene, the number of transcripts of which increased in the roots by 16 times as compared to the control (Figure 3). The *StLOX* protein was localized in the underground parts (roots and tubers) of the potato, as evidenced by the additional proteomic analysis of lipoxygenases in individual organs (Supplementary Table S3). A decrease in α -ketols was observed (Figure 9B), especially derived from 9-HPOT (3 times compared to the control). In shoots, the number of hydroperoxides did not change due to darkness. Darkness led to the appearance of 9-oxononanoic acid, as well as the accumulation of 9,10-epoxy-11-hydroxy-12-octadecenoic acid (9-EAS product) in shoots. The accumulation of the 9-EAS product is consistent with the increased expression of the *StHPL/EAS* gene in shoots (Figure 3A). As we described earlier, the *StHPL/EAS* enzyme exhibits double hydroperoxide lyase/epoxyalcohol synthase activity [74].

Oxidative stress led to slight increase in the amount of 9-HPOD in shoots (Figure 9C). Moreover, there was an increase in 9-oxononanoic acid and 9,10-epoxy-11-hydroxy-12-octadecenoic acid (9-EAS product) synthesized from 9-HPOD, which is consistent with increased expression of the *StHPL/EAS* gene. In roots (Figure 10C), oxidative stress also led to a slight increase in the amount of 9-HPOD, as well as a change in the ratio of the number of α -ketols compared to the control. α -Ketol synthesized from 9-HPOD increased (**5a/5b**), while the peak of α -ketol synthesized from 9-HPOT became smaller (**6a/6b**) (Figure 10C).

Analysis of the oxylipin profile of shoot and root samples after NaCl treatment did not reveal a significant difference from the control (Supplementary Figure S4). Interestingly, the DES products were not detected in any sample, which was also the case for the 13-HPL products. The absence of these oxylipins among the analyzed products is due to the fact that they are involved in defense reactions during attacks of pathogens (biotic stress), such as infections caused by *Pectobacterium atrosepticum* [29].

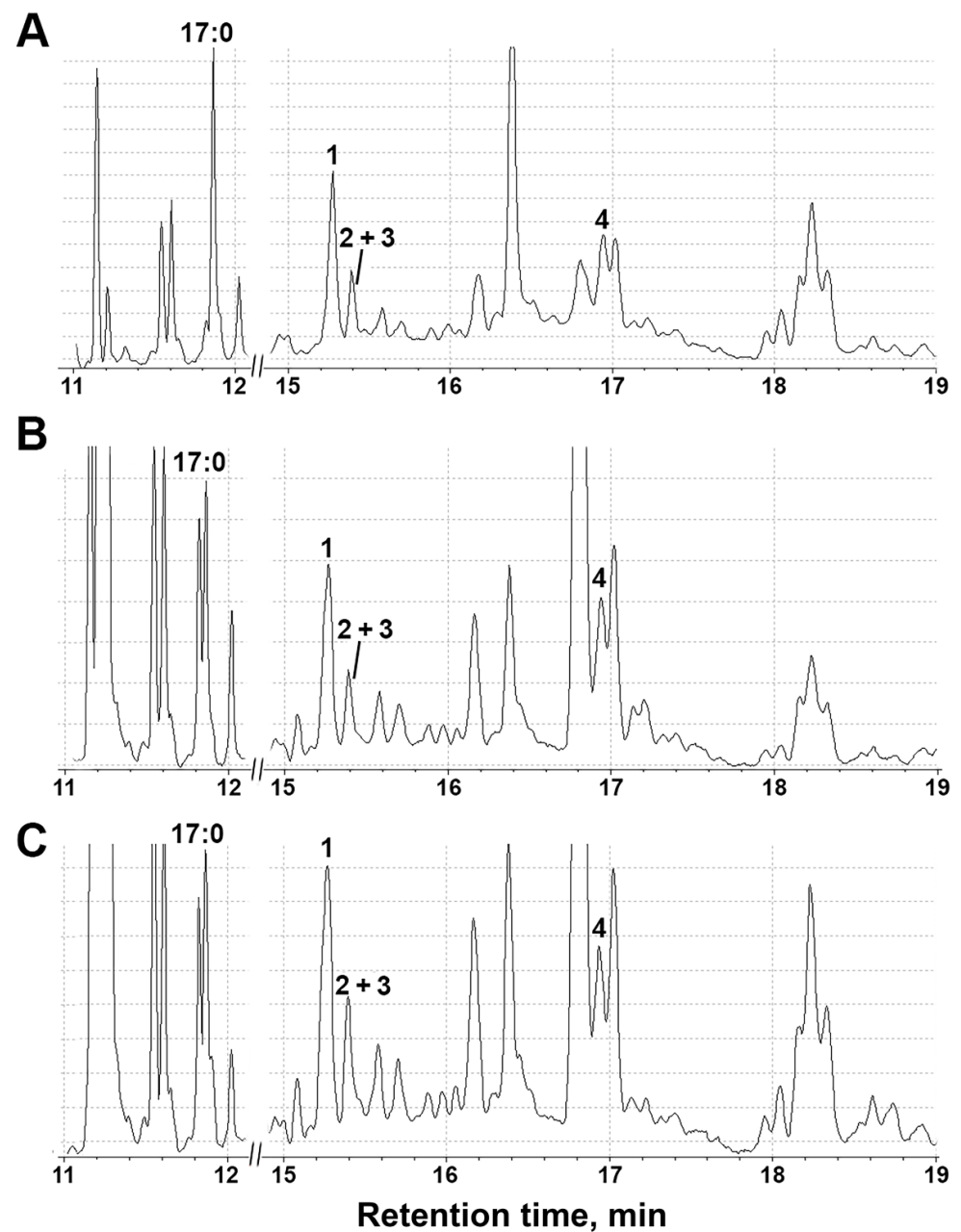


Figure 9. The total ion current (TIC) GC-MS chromatograms of lipoxxygenase cascade products (Me/TMS) in *S. tuberosum* shoot extracts after incubation with linoleic and α -linolenic acids: (A) control plants; (B) plants during darkness; and (C) plants under oxidative stress. **1:** (9*S*,10*E*,12*Z*)-9-hydroxy-10,12-octadecadienoic acid (9-HOD, derivative of 9-LOX product); **2:** (9*S*,10*E*,12*Z*,15*Z*)-9-hydroxy-10,12,15-octadecatrienoic acid (9-HOT, derivative of 9-LOX product); **3:** 13-HOD + 13-HOT, **4:** 9,10-epoxy-11-hydroxy-12-octadecenoic acid (9-EAS product). 17:0: margaric acid (internal standard).

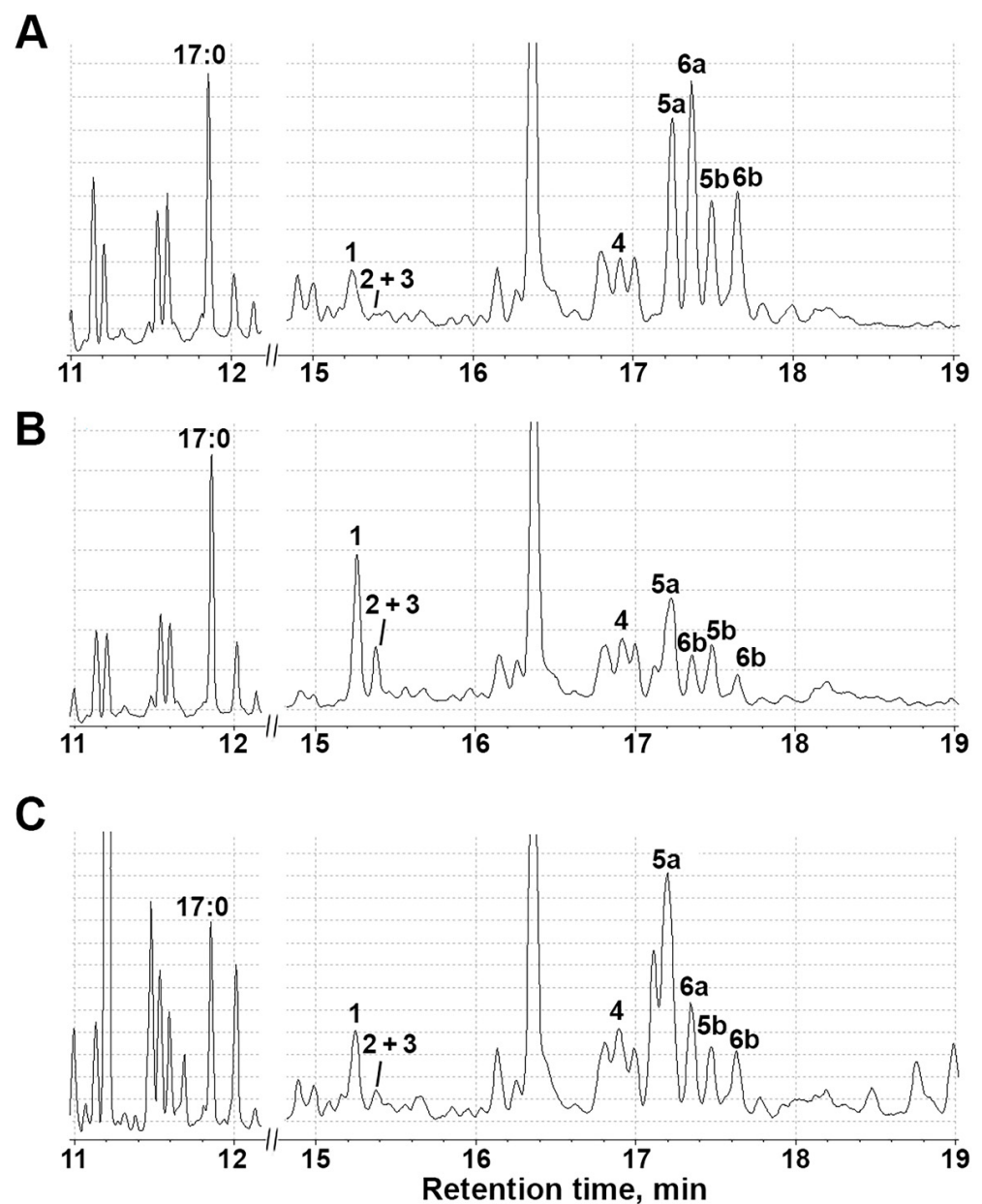


Figure 10. The TIC GC-MS chromatograms of lipoxygenase cascade products (Me/TMS) in *S. tuberosum* root extracts after incubation with linoleic and α -linolenic acids: (A) control plants; (B) plants under during darkness; and (C) plants after treatment with paraquat. 1: 9-HOD (derivative of 9-LOX product); 2: 9-HOT (derivative of 9-LOX product); 3: 13-HOD + 13-HOT; 4: 9,10-epoxy-11-hydroxy-12-octadecenoic acid (9-EAS product); 5a and 5b: *threo* and *erythro* isomers of 9,10-dihydroxy-12-octadecenoic acid (*vic*-diols formed the NaBH₄ reduction in alpha-ketol, 9-AOS product of 9-HPOD conversion); 6a and 6b: *threo* and *erythro* isomers of 9,10-dihydroxy-12,15-octadecadienoic acid (*vic*-diols formed the NaBH₄ reduction in alpha-ketol, 9-AOS product of 9-HPOT conversion).

3. Materials and Methods

3.1. Plant Growth Conditions and Stress

Potato (*Solanum tuberosum* L.) variety Zhukovskiy ranniy (Greenvale AP Ltd., Cambs, UK) was used in the present study. Potato plants were grown axenically in tubes in a growth chamber with a 16 h light/8 h dark cycle in Murashige and Skoog medium [75]. After 30 days of sowing, potato seedlings were subjected to several types of stress: darkness, salinity and herbicide toxicity.

Salinity was caused by NaCl treatments (25, 50 and 100 mM). After 1, 4 and 14 days, the plants were harvested for further analyses. Herbicide toxicity was investigated using paraquat (1,1-dimethyl-4,4-bipyridinium dichloride) (10^{-5} and 10^{-6} M). After 1, 2, 4 and 6 h, the plants were harvested for further analysis. Darkness was ensured by transferring 20-day-old potato seedlings into the dark and maturing them there. Samples for analysis were taken on days 1, 2, 3, 5 and 7. A minimum of three biological replicates were used for each time point, and each biological replicate comprised material pooled from several plants.

3.2. RNA Extraction and cDNA Synthesis

Potato shoots (stems including their appendages, leaves and lateral buds) and roots were ground to a fine powder in liquid nitrogen, and total RNA samples were then extracted using the RNeasy Plant Mini kit (Qiagen, Hilden, Germany) with the processing step of DNase according to the manufacturer's instructions. RNA quantity and quality were confirmed with a NanoDrop ND-1000 spectrophotometer (NanoDrop, Hampton, NH, USA) and 1% agarose gel electrophoresis. Total RNA (1 µg) was converted to cDNA with M-MuLV Reverse Transcriptase (Fermentas, Vilnius, Lithuania), according to the standard protocol from the manufacturer.

3.3. Quantitative Real-Time PCR (qRT-PCR)

Quantitative real-time PCR was carried out on a CFX96 Touch Real-Time PCR Detection System (Bio-Rad, Hercules, CA, USA) using $2.5\times$ EVA Green master mix (Syntol, Moscow, Russia). Primers were designed using the Vector NTI Advance 11.5 program (Invitrogen, Waltham, MA, USA), according to the gene sequences in the GenBank and Phytozome Database. The specific primer pairs are shown in Supplementary Table S1. The PCR mixture contained $1\times$ EVA Green master mix, $0.4\ \mu\text{M}$ of each forward and reverse primer, cDNA and DNase free water for a total volume of $10\ \mu\text{L}$. The thermal profile of the real-time system was one step at $95\ ^\circ\text{C}$ for 2 min, followed by 40 cycles at $94\ ^\circ\text{C}$ for 10 s (denaturation) and at $60\ ^\circ\text{C}$ for 15 s (annealing), $72\ ^\circ\text{C}$ for 30 s (extension), followed by adding a $60\text{--}95\ ^\circ\text{C}$ melting curve to confirm specificity of the products. From each of three biologically independent cDNA samples, two independent technical replications were performed, and averaged for further calculations. Relative transcript abundance calculations were performed using the CFX Maestro software (Bio-Rad, Hercules, CA, USA). In the work, the normalized gene expression ($\Delta\Delta\text{Cq}$) was calculated. The significance of the differences in results was determined using Student's *t*-test. $p < 0.05$ was considered statistically significant. The data are presented as means \pm SD.

3.4. Bioinformatics Methods

Amino acid and nucleotide sequences of CYP74 enzymes of *S. tuberosum* were taken from NCBI and Phytozome databases for phylogenetic analysis and illustrations of exon–intron organization genes. The multiple alignments of CYP74 amino acid sequences were carried out with MEGA7 software [76]. The phylogenetic tree of CYP74s was inferred using the maximum likelihood method based on the Poisson correction model [77]. The resulting phylogenetic data and gene characteristics were visualized using the Gene Structure Display Server (GSDS) [78].

The promoter sequences (1 kb upstream regions to the start codon) of target genes were retrieved from the potato genome sequence v4.03 from Phytozome database (<http://www.phytozome.net/> accessed on 10 January 2022). The tools PlantCare (<http://bioinformatics.psb.ugent.be/webtools/plantcare/html/> accessed on 10 January 2022 [79] and PLACE (<https://www.dna.affrc.go.jp/PLACE/?action=newplace> accessed on 10 January 2022) were used for the identification of *cis*-regulatory elements in promoters of *S. tuberosum* CYP74 genes.

3.5. Profiling of *S. tuberosum* Oxylipins under Abiotic Stresses

The *S. tuberosum* samples of tissues (shoots and roots, 2 g fresh weight) were homogenized in liquid nitrogen. After adding 4 mL of ice-cold 50 mM Tris-HCl buffer, pH 7.0, the samples were filtered through cheesecloth and incubated with 150 µg linoleic, 150 µg α -linolenic and 75 µg margaric (internal standard) acids at 23 °C for 30 min under continuous oxygen bubbling. The reaction mixture was acidified to pH 6.0 and the reaction products were extracted with a 10 mL mixture of ethyl acetate/hexane (1:1, by volume) as described previously [47]. Then, the resulting products were methylated with ethereal diazomethane and trimethylsilylated with pyridine/hexamethyldisilazane/trimethylchlorosilane (1:1:1, by volume) mixture at 23 °C for 30 min. Additionally, the products were reduced with NaBH₄, and then methylated and trimethylsilylated. The silylation reagents were evaporated in vacuo, and dissolved in 100 µL of hexane. The obtained product derivatives (methyl esters/trimethylsilyl derivatives (Me/TMS)) were analyzed by GC-MS.

The GC-MS analyses were performed using a Shimadzu QP2020A mass spectrometer connected to Shimadzu GC-2010 Plus gas chromatograph equipped with a Macherey-Nagel Optima-5-MS (5% phenyl 95% methylpolysiloxane) fused capillary column (length, 30 m; ID 0.25 mm; film thickness, 0.25 µm) (Shimadzu, Kyoto, Japan). Helium at a flow rate of 30 cm/s was used as the carrier gas. Injections were performed in the split mode using an initial column temperature of 120 °C, with injector temperature of 230 °C. Then, the column temperature was raised at 10 °C/min until 240 °C. Electron impact ionization (70 eV) was used.

4. Conclusions

In higher plants, the most common C18 polyene fatty acids are 18:1 (oleate), 18:2 (linoleate) and 18:3 (α -linolenate) [80]. The suppression of the expression of a number of genes of the lipoxygenase cascade, in addition to the redistribution of signaling functions, may be due to the transfer of the main substrates (C18 fatty acids) from the biosynthesis of oxylipins to the formation of protective biopolymers (cutin and suberin), which are also derivatives of fatty acids [81]. This is confirmed by the literature data showing that the monomeric composition of cutin or suberin can vary greatly depending on the type of plant, organ and stage of development. In Arabidopsis, for example, the cutin of leaves and stems has an unusually high content of dicarboxylic acids derived from 18:2 [82], while the cutin of flowers is mainly composed of dihydroxy acids derived from 16:0 [83]. In addition, there are other protective biopolymers consisting of aliphatic and aromatic hydrocarbons such as cutane. It is present in some plants as an additional cuticle fraction [84], with a ratio of 18:2 apparently preferred as a building block over 16:0 [85].

Interestingly, both under abiotic and biotic stresses, activation of the 9-LOX pathway was detected. However, in the case of biotic stress in cultured potato cells treated with elicitor from *Phytophthora infestans*, the accumulation of colneleic acid (a product of the 9-DES branch of the LOX pathway) was detected [86]. A similar result was observed in tobacco (*Nicotiana tabacum*) plants, where the impact of the elicitor or pathogen led to the accumulation of colneleic and colnelenic acids [87]. Thus, different types of stress factors can lead to the same intermediate products (in this case, 9-HPOD), which are then utilized by different CYP74 enzymes. Significant changes in the profiles of oxylipins were related to the transformation of 9-HPOD in 9-AOS and 9-EAS pathways (Figures 9 and 10). Since all CYP74 enzymes of potato have been characterized, 9-EAS products can be formed only by StHPL/EAS, which also exhibits HPL activity, and is able to convert not only 9- but also 13-hydroperoxides [74].

The obtained data on the lipoxygenase system complement the multiplicity of interactions between signaling systems that directly or indirectly link biosynthesis, perception and signaling of various phytohormones. The final formation of oxylipins will depend not only on the activation of certain genes, but more importantly the presence of specific CYP74 enzymes (AOS, DES, HPL, EAS, etc.) and the availability of substrates, since some CYP74 enzymes have cytosolic localization and some are membrane-associated. Therefore,

in violation of the integrity of tissues, de novo formation of oxylipins can occur without the activation of certain genes, but only due to the availability of the substrate. Along with this, it is obvious that the signaling pathways do not function separately, but are cross-regulated, leading to plant adaptation to current conditions. Preactivation of one resistance mechanism can increase plant resistance to a number of factors. The results obtained during this study expand knowledge of a vast and diverse group of plant metabolites, oxylipins, which not only participate in the defense mechanisms of plants, but also determine the number of valuable organoleptic properties of plants. For example, the volatile C6 and C9 compounds (green leaf volatiles) of the hydroperoxide lyase branch impart aromas and flavors to many vegetables and fruits. Further study of already known key players and the identification of new components in phytohormone interaction networks will expand understanding of the mechanisms underlying the delicate balance of plant growth and development and their defense responses.

Supplementary Materials: The following supporting information can be downloaded at: <https://www.mdpi.com/article/10.3390/plants11050683/s1>, Figure S1: Changes in marker gene expression of other signaling pathways in response to treatment with NaCl (25 and 50 mM) in shoots and roots; Figure S2: The electron impact mass spectrum of compounds 5a (vic-diol) and the corresponding mass fragmentation scheme; Figure S3: The electron impact mass spectrum of compounds 6a (vic-diol) and the corresponding mass fragmentation scheme; Figure S4: The total ion current (TIC) GC-MS chromatograms of lipoxygenase cascade products (Me/TMS) in *S. tuberosum* shoot extracts after incubation with linoleic and α -linolenic acids: (A) shoots after NaCl treatment; (B) roots after NaCl treatment; Table S1: Primers for qRT-PCR amplification.; Table S2: List of marker genes for different hormonal systems; and Table S3: Identified lipoxygenase (StLOX) in underground potato organs.

Author Contributions: Conceptualization, S.G. and Y.T.; methodology, S.G., A.O. and L.M.; software, S.G.; formal analysis, Y.T.; investigation, S.G., A.O. and L.M.; writing—original draft preparation, S.G.; writing—review and editing, S.G. and Y.T.; and visualization, S.G. All authors have read and agreed to the published version of the manuscript.

Funding: The authors are thankful for the financial support from the government assignment for FRC Kazan Scientific Center of RAS (bioinformatic and phylogenetic analyses). S.G. thanks the Grants Council of the President of the Russian Federation (MK-903.2020.4) for financial support (studies of the dynamics of gene expression). L.M. thanks the Russian Science Foundation (project no. 21-14-00397) for financial support (study of lipoxygenase cascade).

Institutional Review Board Statement: Not applicable.

Informed Consent Statement: Not applicable.

Data Availability Statement: All the data are available in the manuscript and Supplementary Materials.

Acknowledgments: The authors thank Alevtina Egorova for protein analyses and the skillful technical assistance at separate stages of the experiments.

Conflicts of Interest: The authors declare no conflict of interest.

References

1. Mosblech, A.; Feussner, I.; Heilmann, I. Oxylipins: Structurally diverse metabolites from fatty acid oxidation. *Plant Physiol. Biochem.* **2009**, *47*, 511–517. [[CrossRef](#)] [[PubMed](#)]
2. Wasternack, C.; Feussner, I. The Oxylipin Pathways: Biochemistry and Function. *Annu. Rev. Plant Biol.* **2018**, *69*, 363–386. [[CrossRef](#)]
3. Christensen, S.A.; Huffaker, A.; Kaplan, F.; Sims, J.; Ziemann, S.; Doehlemann, G.; Ji, L.; Schmitz, R.J.; Kolomiets, M.V.; Alborn, H.T.; et al. Maize death acids, 9-lipoxygenase-derived cyclopent(a)nonenes, display activity as cytotoxic phytoalexins and transcriptional mediators. *Proc. Natl. Acad. Sci. USA* **2015**, *112*, 11407–11412. [[CrossRef](#)] [[PubMed](#)]
4. Christensen, S.A.; Huffaker, A.; Hunter, C.T.; Alborn, H.T.; Schmelz, E.A. A maize death acid, 10-oxo-11-phytoenoic acid, is the predominant cyclopentenone signal present during multiple stress and developmental conditions. *Plant Signal. Behav.* **2016**, *11*, e1120395. [[CrossRef](#)] [[PubMed](#)]
5. Griffiths, G. Jasmonates: Biosynthesis, perception and signal transduction. *Essays Biochem.* **2020**, *64*, 501–512. [[CrossRef](#)]

6. Matsui, K. Green leaf volatiles: Hydroperoxide lyase pathway of oxylipin metabolism. *Curr. Opin. Plant Biol.* **2006**, *9*, 274–280. [[CrossRef](#)]
7. Bottcher, C.; Weiler, E.W. cyclo-Oxylipin-galactolipids in plants: Occurrence and dynamics. *Planta* **2007**, *226*, 629–637. [[CrossRef](#)]
8. Farag, M.A.; Fokar, M.; Abd, H.; Zhang, H.; Allen, R.D.; Paré, P.W. (Z)-3-Hexenol induces defense genes and downstream metabolites in maize. *Planta* **2005**, *220*, 900–909. [[CrossRef](#)]
9. Frost, C.J.; Mescher, M.C.; Dervinis, C.; Davis, J.M.; Carlson, J.E.; De Moraes, C.M. Priming defense genes and metabolites in hybrid poplar by the green leaf volatile *cis*-3-hexenyl acetate. *New Phytol.* **2008**, *180*, 722–734. [[CrossRef](#)]
10. Croft, K.; Juttner, F.; Slusarenko, A.J. Volatile Products of the Lipoxygenase Pathway Evolved from *Phaseolus vulgaris* (L.) Leaves Inoculated with *Pseudomonas syringae* pv *phaseolicola*. *Plant Physiol.* **1993**, *101*, 13–24. [[CrossRef](#)]
11. Nakamura, S.; Hatanaka, A.J. Green-leaf-derived C6-aroma compounds with potent antibacterial action that act on both Gram-negative and Gram-positive bacteria. *J. Agric. Food. Chem.* **2002**, *50*, 7639–7644. [[CrossRef](#)] [[PubMed](#)]
12. Hamilton-Kemp, T.R.; McCracken, C.T., Jr.; Loughrin, J.H.; Andersen, R.A.; Hildebrand, D.F. Effects of some natural volatile compounds on the pathogenic fungi *Alternaria alternata* and *Botrytis cinerea*. *J. Chem. Ecol.* **1992**, *18*, 1083–1091. [[CrossRef](#)] [[PubMed](#)]
13. Kallenbach, M.; Gilardoni, P.A.; Allmann, S.; Baldwin, I.T.; Bonaventure, G. C12 derivatives of the hydroperoxide lyase pathway are produced by product recycling through lipoxygenase-2 in *Nicotiana attenuata* leaves. *New Phytol.* **2011**, *191*, 1054–1068. [[CrossRef](#)]
14. Stumpe, M.; Kandzia, R.; Göbel, C.; Rosahl, S.; Feussner, I. A pathogen-inducible divinyl ether synthase (CYP74D) from elicitor-treated potato suspension cells. *FEBS Lett.* **2001**, *507*, 371–376. [[CrossRef](#)]
15. Gorina, S.S.; Toporkova, Y.Y.; Mukhtarova, L.S.; Chechetkin, I.R.; Khairutdinov, B.I.; Gogolev, Y.V.; Grechkin, A.N. Detection and molecular cloning of CYP74Q1 gene: Identification of *Ranunculus acris* leaf divinyl ether synthase. *Biochim. Biophys. Acta* **2014**, *1841*, 1227–1233. [[CrossRef](#)] [[PubMed](#)]
16. Gorina, S.S.; Toporkova, Y.Y.; Mukhtarova, L.S.; Smirnova, E.O.; Chechetkin, I.R.; Khairutdinov, B.I.; Gogolev, Y.V.; Grechkin, A.N. Oxylipin biosynthesis in spikemoss *Selaginella moellendorffii*: Molecular cloning and identification of divinyl ether synthases CYP74M1 and CYP74M3. *Biochim. Biophys. Acta* **2016**, *1861*, 301–309. [[CrossRef](#)]
17. Toporkova, Y.Y.; Smirnova, E.O.; Gorina, S.S.; Mukhtarova, L.S.; Grechkin, A.N. Detection of the first higher plant epoxyalcohol synthase: Molecular cloning and characterisation of the CYP74M2 enzyme of spikemoss *Selaginella moellendorffii*. *Phytochemistry* **2018**, *156*, 73–82. [[CrossRef](#)]
18. Toporkova, Y.Y.; Bessolitsyna, E.K.; Smirnova, E.O.; Gorina, S.S.; Petrova, O.E.; Mukhtarova, L.S.; Grechkin, A.N. Antimicrobial Activity of Geometric Isomers of Etherolenic Acid—the Products of Plant Lipoxygenase Cascade. *Dokl. Biochem. Biophys.* **2018**, *480*, 139–142. [[CrossRef](#)]
19. Weber, H.; Chetelat, A.; Caldelari, D.; Farmer, E.E. Divinyl ether fatty acid synthesis in late blight-diseased potato leaves. *Plant Cell* **1999**, *11*, 485–493. [[CrossRef](#)]
20. Graner, G.; Hamberg, M.; Meijer, J. Screening of oxylipins for control of oilseed rape (*Brassica napus*) fungal pathogens. *Phytochemistry* **2003**, *63*, 89–95. [[CrossRef](#)]
21. Nelson, D.R.; Goldstone, J.V.; Stegeman, J.J. The cytochrome P450 genesis locus: The origin and evolution of animal cytochrome P450s. *Philos. Trans. R. Soc. Lond. B Biol. Sci.* **2013**, *368*, 20120474. [[CrossRef](#)] [[PubMed](#)]
22. Birch, P.R.J.; Bryan, G.; Fenton, B.; Gilroy, E.M.; Hein, I.; Jones, J.T.; Prashar, A.; Taylor, M.A.; Torrance, L.; Toth, I.K. Crops that feed the world 8: Potato: Are the trends of increased global production sustainable. *Food Secur.* **2012**, *4*, 477–508. [[CrossRef](#)]
23. Machida-Hirano, R. Diversity of potato genetic resources. *Breed Sci.* **2015**, *65*, 26–40. [[CrossRef](#)]
24. Zaheer, K.; Akhtar, M.H. Potato Production, Usage, and Nutrition—A Review. *Crit. Rev. Food. Sci. Nutr.* **2016**, *56*, 711–721. [[CrossRef](#)]
25. Fujii, S.; Kobayashi, K.; Nakamura, Y.; Wada, H. Inducible knockdown of *MONOGALACTOSYLDIACYLGLYCEROL SYNTHASE1* reveals roles of galactolipids in organelle differentiation in *Arabidopsis* cotyledons. *Plant Physiol.* **2014**, *166*, 1436–1449. [[CrossRef](#)] [[PubMed](#)]
26. Armarego-Marriott, T.; Sandoval-Ibañez, O.; Kowalewska, Ł. Beyond the darkness: Recent lessons from etiolation and de-etiolation studies. *J. Exp. Bot.* **2020**, *71*, 1215–1225. [[CrossRef](#)] [[PubMed](#)]
27. Jacq, A.; Pernot, C.; Martinez, Y.; Domergue, F.; Payré, B.; Jamet, E.; Burlat, V.; Pacquit, V.B. The *Arabidopsis* Lipid Transfer Protein 2 (AtLTP2) Is Involved in Cuticle-Cell Wall Interface Integrity and in Etiolated Hypocotyl Permeability. *Front. Plant Sci.* **2017**, *8*, 263. [[CrossRef](#)]
28. Ziegler, J.; Stenzel, I.; Hause, B.; Maucher, H.; Miersch, O.; Hamberg, M.; Grimm, M.; Ganai, M.; Wasternack, C. Molecular cloning of allene oxide cyclase: The enzyme establishing the stereochemistry of octadecanoids and jasmonates. *J. Biol. Chem.* **2000**, *275*, 19132–19138. [[CrossRef](#)]
29. Wasternack, C.; Hause, B. Jasmonates and octadecanoids: Signals in plant stress responses and plant development. *Prog. Nucl. Acid Res.* **2002**, *72*, 165–221. [[CrossRef](#)]
30. Stenzel, I.; Hause, B.; Maucher, H.; Pitzschke, A.; Miersch, O.; Ziegler, J.; Ryan, C.A.; Wasternack, C. Allene oxide cyclase dependence of the wound response and vascular bundle-specific generation of jasmonates in tomato—Amplification in wound signaling. *Plant J.* **2003**, *33*, 577–589. [[CrossRef](#)]

31. Gasperini, D.; Chauvin, A.; Acosta, I.F.; Kurenda, A.; Stolz, S.; Chételat, A.; Wolfender, J.L.; Farmer, E.E. Axial and Radial Oxylinp Transport. *Plant Physiol.* **2015**, *169*, 2244–2254. [[CrossRef](#)] [[PubMed](#)]
32. Chen, Q.; Sun, J.; Zhai, Q.; Zhou, W.; Qi, L.; Xu, L.; Wang, B.; Chen, R.; Jiang, H.; Qi, J.; et al. The Basic Helix-Loop-Helix Transcription Factor MYC2 Directly Represses PLETHORA Expression during Jasmonate-Mediated Modulation of the Root Stem Cell Niche in Arabidopsis. *Plant Cell* **2011**, *23*, 3335–3352. [[CrossRef](#)] [[PubMed](#)]
33. Zhu, Z.; Lee, B. Friends or foes: New insights in jasmonate and ethylene co-actions. *Plant Cell Physiol.* **2015**, *56*, 414–420. [[CrossRef](#)] [[PubMed](#)]
34. Pauwels, L.; Ritt, A.; Goossens, J.; Durand, A.N.; Liu, H.; Gu, Y.; Geerinck, J.; Boter, M.; Vanden Bossche, R.; De Clercq, R.; et al. Ring E3 Ligase keep on going modulates JASMONATE ZIM-DOMAIN12 Stability. *Plant Physiol.* **2015**, *169*, 1405–1417. [[CrossRef](#)] [[PubMed](#)]
35. Shim, J.S.; Jung, C.; Lee, S.; Min, K.; Lee, Y.W.; Choi, Y.; Lee, J.S.; Song, J.T.; Kim, J.K.; Choi, Y.D. AtMYB44 regulates WRKY70 expression and modulates antagonistic interaction between salicylic acid and jasmonic acid signaling. *Plant J.* **2013**, *73*, 483–495. [[CrossRef](#)] [[PubMed](#)]
36. Wasternack, C.; Hause, B. Jasmonates: Biosynthesis, perception, signal transduction and action in plant stress response, growth and development. An update to the 2007 review in *Annals of Botany*. *Ann. Bot.* **2013**, *111*, 1021–1058. [[CrossRef](#)]
37. Harris, N.; Taylor, J.E.; Roberts, J.A. Characterization and expression of an mRNA encoding a wound-induced (Win) protein from ethylene-treated tomato leaf abscission zone tissue. *J. Exp. Bot.* **1997**, *48*, 1223–1227. [[CrossRef](#)]
38. Humplík, J.F.; Turečková, V.; Fellner, M.; Bergougnoux, V. Spatio-temporal changes in endogenous abscisic acid contents during etiolated growth and photomorphogenesis in tomato seedlings. *Plant Signal. Behav.* **2015**, *10*, e1039213. [[CrossRef](#)]
39. Humplík, J.F.; Bergougnoux, V.; Van Volkenburgh, E. To Stimulate or Inhibit? That Is the Question for the Function of Abscisic Acid. *Trends Plant Sci.* **2017**, *22*, 830–841. [[CrossRef](#)]
40. Reid, J.B.; Botwright, N.A.; Smith, J.J.; O’Neill, D.P.; Kerckhoffs, L.H. Control of Gibberellin Levels and Gene Expression during De-Etiolation in Pea. *Plant Physiol.* **2002**, *128*, 734–741. [[CrossRef](#)]
41. Yoshida, Y.; Sano, R.; Wada, T.; Takabayashi, J.; Okada, K. Jasmonic acid control of GLABRA3 links inducible defense and trichome patterning in Arabidopsis. *Development* **2009**, *136*, 1039–1048. [[CrossRef](#)] [[PubMed](#)]
42. Hou, X.; Lee, L.Y.; Xia, K.; Yan, Y.; Yu, H. DELLAs modulate jasmonate signaling via competitive binding to JAZs. *Dev. Cell.* **2010**, *19*, 884–894. [[CrossRef](#)] [[PubMed](#)]
43. Yang, D.L.; Yao, J.; Mei, C.S.; Tong, X.H.; Zeng, L.J.; Li, Q.; Xiao, L.T.; Sun, T.P.; Li, J.; Deng, X.W.; et al. Plant hormone jasmonate prioritizes defense over growth by interfering with gibberellin signaling cascade. *Proc. Natl. Acad. Sci. USA* **2012**, *109*, E1192–E1200. [[CrossRef](#)] [[PubMed](#)]
44. Lascano, R.; Muñoz, N.; Robert, G.; Rodriguez, M.; Melchiorre, M.; Trippi, V.; Quero, G. Paraquat: An Oxidative Stress Inducer. In *Herbicides—Properties, Synthesis and Control of Weeds*; Hasaneen, M.N., Ed.; InTech: Rijeka, Croatia, 2012; pp. 135–148.
45. Yan, Y.; Stolz, S.; Chételat, A.; Reymond, P.; Pagni, M.; Dubugnon, L.; Farmer, E.E. A Downstream Mediator in the Growth Repression Limb of the Jasmonate Pathway. *Plant Cell* **2007**, *19*, 2470–2483. [[CrossRef](#)]
46. Chini, A.; Fonseca, S.; Fernández, G.; Adie, B.; Chico, J.M.; Lorenzo, O.; García-Casado, G.; López-Vidriero, I.; Lozano, F.M.; Ponce, M.R.; et al. The JAZ family of repressors is the missing link in jasmonate signalling. *Nature* **2007**, *448*, 666–671. [[CrossRef](#)]
47. Gorshkov, V.Y.; Toporkova, Y.Y.; Tseris, I.D.; Smirnova, E.O.; Ogorodnikova, A.V.; Gogoleva, N.E.; Parfirova, O.I.; Petrova, O.E.; Gogolev, Y.V. Differential modulation of the lipoxygenase cascade during typical and latent *Pectobacterium atrosepticum* infections. *Ann. Bot.* **2022**, *129*, 271–286. [[CrossRef](#)]
48. Chini, A.; Ben-Romdhane, W.; Hassairi, A.; Aboul-Soud, M.A.M. Identification of TIFY/JAZ family genes in *Solanum lycopersicum* and their regulation in response to abiotic stresses. *PLoS ONE* **2017**, *12*, e0177381. [[CrossRef](#)]
49. Zhu, D.; Li, R.; Liu, X.; Sun, M.; Wu, J.; Zhang, N.; Zhu, Y. The Positive Regulatory Roles of the TIFY10 Proteins in Plant Responses to Alkaline Stress. *PLoS ONE* **2014**, *9*, e111984. [[CrossRef](#)]
50. Zhu, D.; Bai, X.; Chen, C.; Chen, Q.; Cai, H.; Li, Y.; Ji, W.; Zhai, H.; Lv, D.; Luo, X.; et al. GsTIFY10, a novel positive regulator of plant tolerance to bicarbonate stress and a repressor of jasmonate signaling. *Plant Mol. Biol.* **2011**, *77*, 285–297. [[CrossRef](#)]
51. Nambara, E.; Marion-Poll, A. Abscisic acid biosynthesis and catabolism. *Annu. Rev. Plant Biol.* **2005**, *56*, 165–185. [[CrossRef](#)]
52. Guajardo, E.; Correa, J.A.; Contreras-Porcia, L. Role of abscisic acid (ABA) in activating antioxidant tolerance responses to desiccation stress in intertidal seaweed species. *Planta* **2016**, *243*, 767–781. [[CrossRef](#)] [[PubMed](#)]
53. Wakeel, A.; Ali, I.; Wu, M.; Kkan, A.R.; Jan, M.; Ali, A.; Liu, Y.; Ge, S.; Wu, J.; Liu, B.; et al. Ethylene mediates dichromate-induced oxidative stress and regulation of the enzymatic antioxidant system-related transcriptome in Arabidopsis thaliana. *Environ. Exp. Bot.* **2018**, *161*, 166–179. [[CrossRef](#)]
54. Sewelam, N.; Kazan, K.; Thomas-Hall, S.R.; Kidd, B.N.; Manners, J.M.; Schenk, P.M. Ethylene Response Factor 6 Is a Regulator of Reactive Oxygen Species Signaling in Arabidopsis. *PLoS ONE* **2013**, *8*, e70289. [[CrossRef](#)] [[PubMed](#)]
55. Yao, Y.; He, R.J.; Xie, Q.L.; Zhao, X.H.; Deng, X.M.; He, J.B.; Song, L.; He, J.; Marchant, A.; Chen, X.Y.; et al. ETHYLENE RESPONSE FACTOR 74 (ERF74) plays an essential role in controlling a respiratory burst oxidase homolog D (RbohD)-dependent mechanism in response to different stresses in Arabidopsis. *New Phytol.* **2017**, *213*, 1667–1681. [[CrossRef](#)] [[PubMed](#)]
56. Ivushkin, K.; Bartholomeus, H.; Bregt, A.K.; Pulatov, A.; Kempen, B.; De Sousa, L. Global mapping of soil salinity change. *Remote Sens. Environ.* **2019**, *231*, 111260. [[CrossRef](#)]

57. Stumpe, M.; Göbel, C.; Demchenko, K.; Hoffmann, M.; Klösigen, R.B.; Pawlowski, K.; Feussner, I. Identification of an allene oxide synthase (CYP74C) that leads to formation of alpha-ketols from 9-hydroperoxides of linoleic and linolenic acid in below-ground organs of potato. *Plant J.* **2006**, *47*, 883–896. [[CrossRef](#)]
58. Farmaki, T.; Sanmartín, M.; Jiménez, P.; Paneque, M.; Sanz, C.; Vancanneyt, G.; León, J.; Sánchez-Serrano, J.J. Differential distribution of the lipoxygenase pathway enzymes within potato chloroplasts. *J. Exp. Bot.* **2007**, *58*, 555–568. [[CrossRef](#)]
59. Zhao, Y.; Dong, W.; Zhang, N.; Ai, X.; Wang, M.; Huang, Z.; Xiao, L.; Xia, G. A Wheat Allene Oxide Cyclase Gene Enhances Salinity Tolerance via Jasmonate Signaling. *Plant Physiol.* **2014**, *164*, 1068–1076. [[CrossRef](#)]
60. Chen, X.; Zhang, X.; Jia, A.; Xu, G.; Hu, H.; Hu, X.; Hu, L. Jasmonate mediates salt-induced nicotine biosynthesis in tobacco (*Nicotiana tabacum* L.). *Plant Divers.* **2016**, *38*, 118–123. [[CrossRef](#)]
61. Wasternack, C.; Song, S. Jasmonates: Biosynthesis, metabolism, and signaling by proteins activating and repressing transcription. *J. Exp. Bot.* **2017**, *68*, 1303–1321. [[CrossRef](#)]
62. Hilda, R.; Graciela, A.; Sergio, M.; Otto, R.; Ingrid, P.C.; Hugo, T.; Edith, M.D.; Estela, A. Guillermina. Salt tolerant tomato plants show increased levels of jasmonic acid. *Plant Growth Regul.* **2003**, *41*, 149–158.
63. Filgueiras, C.C.; Martins, A.D.; Pereira, R.V.; Willett, D.S. The ecology of salicylic acid signaling: Primary, secondary and tertiary effects with applications in agriculture. *Int. J. Mol. Sci.* **2019**, *20*, 5851. [[CrossRef](#)] [[PubMed](#)]
64. Khan, A.; Kamran, M.; Imran, M.; Al-Harrasi, A.; Al-Rawahi, A.; Al-Amri, I.; Lee, I.J.; Khan, A.L. Silicon and salicylic acid confer high-pH stress tolerance in tomato seedlings. *Sci. Rep.* **2019**, *9*, 19788. [[CrossRef](#)]
65. Ahanger, M.A.; Aziz, U.; Alsahli, A.A.; Alyemeni, M.N.; Ahmad, P. Influence of exogenous salicylic acid and nitric oxide on growth, photosynthesis, and ascorbate-glutathione cycle in salt stressed *Vigna angularis*. *Biomolecules* **2019**, *10*, 42. [[CrossRef](#)] [[PubMed](#)]
66. Min, J.H.; Chung, J.S.; Lee, K.H.; Kim, C. The CONSTANS-like 4 transcription factor, AtCOL4, positively regulates abiotic stress tolerance through an abscisic acid-dependent manner in Arabidopsis. *J. Integr. Plant Biol.* **2015**, *57*, 313–324. [[CrossRef](#)] [[PubMed](#)]
67. Yu, Z.; Duan, X.; Luo, L.; Dai, S.; Ding, Z.; Xia, G. How Plant Hormones Mediate Salt Stress Responses. *Trends Plant Sci.* **2020**, *25*, 1117–1130. [[CrossRef](#)] [[PubMed](#)]
68. Ding, Z.J.; Yan, J.Y.; Li, C.X.; Li, G.X.; Wu, Y.R.; Zheng, S.J. Transcription factor WRKY46 modulates the development of Arabidopsis lateral roots in osmotic/salt stress conditions via regulation of ABA signaling and auxin homeostasis. *Plant J.* **2015**, *84*, 56–69. [[CrossRef](#)]
69. Liu, W.; Li, R.J.; Han, T.T.; Cai, W.; Fu, Z.W.; Lu, Y.T. Salt stress reduces root meristem size by nitric oxide-mediated modulation of auxin accumulation and signaling in Arabidopsis. *Plant Physiol.* **2015**, *168*, 343–356. [[CrossRef](#)]
70. Lu, C.; Chen, M.X.; Liu, R.; Zhang, L.; Hou, X.; Liu, S.; Ding, X.; Jiang, Y.; Xu, J.; Zhang, J.; et al. Abscisic acid regulates auxin distribution to mediate maize lateral root development under salt stress. *Front. Plant Sci.* **2019**, *10*, 716. [[CrossRef](#)]
71. Magome, H.; Yamaguchi, S.; Hanada, A.; Kamiya, Y.; Oda, K. The DDF1 transcriptional activator upregulates expression of a gibberellin-deactivating gene, GA2ox7, under high-salinity stress in Arabidopsis. *Plant J.* **2008**, *56*, 613–626. [[CrossRef](#)]
72. Shan, C.; Mei, Z.; Duan, J.; Chen, H.; Feng, H.; Cai, W. OsGA2ox5, a gibberellin metabolism enzyme, is involved in plant growth, the root gravity response and salt stress. *PLoS ONE* **2014**, *9*, e87110. [[CrossRef](#)] [[PubMed](#)]
73. Weber, H.; Vick, B.A.; Farmer, E.E. Dinor-oxo-phytyldienoic acid: A new hexadecanoid signal in the jasmonate family. *Proc. Natl. Acad. Sci. USA* **1997**, *94*, 10473–10478. [[CrossRef](#)] [[PubMed](#)]
74. Toporkova, Y.Y.; Gorina, S.S.; Bessolitsyna, E.K.; Smirnova, E.O.; Fatykhova, V.S.; Brühlmann, F.; Ilyina, T.M.; Mukhtarova, L.S.; Grechkin, A.N. Double function hydroperoxide lyases/epoxyalcohol synthases (CYP74C) of higher plants: Identification and conversion into allene oxide synthases by site-directed mutagenesis. *Biochim. Biophys. Acta Mol. Cell. Biol. Lipids* **2018**, *1863*, 369–378. [[CrossRef](#)] [[PubMed](#)]
75. Murashige, T.; Skoog, F. A revised medium for rapid growth and bio assays with tobacco tissue cultures. *Physiol. Plant* **1962**, *15*, 473–497. [[CrossRef](#)]
76. Kumar, S.; Stecher, G.; Tamura, K. MEGA7: Molecular Evolutionary Genetics Analysis version 7.0 for bigger datasets. *Mol. Biol. Evol.* **2016**, *33*, 1870–1874. [[CrossRef](#)]
77. Zuckerkandl, E.; Pauling, L. Evolutionary divergence and convergence in proteins. In *Evolving Genes and Proteins*; Bryson, V., Vogel, H.J., Eds.; Academic Press: New York, NY, USA, 1965; pp. 97–166.
78. Bo, H.; Jinpu, J.; An-Yuan, G.; He, Z.; Jingchu, L.; Ge, G. GSDS 2.0: An upgraded gene feature visualization server. *Bioinformatics* **2015**, *31*, 1296–1297. [[CrossRef](#)]
79. Lescot, M.; Déhais, P.; Moreau, Y.; De Moor, B.; Rouzé, P.; Rombauts, S. PlantCARE: A database of plant cis-acting regulatory elements and a portal to tools for in silico analysis of promoter sequences. *Nucleic Acids Res.* **2002**, *30*, 325–327. [[CrossRef](#)]
80. Harwood, J.L. Fatty acid metabolism. *Annu. Rev. Plant Physiol. Plant Mol. Biol.* **1988**, *39*, 101–138. [[CrossRef](#)]
81. He, M.; He, C.Q.; Ding, N.Z. Abiotic stresses: General defenses of land plants and chances for engineering multistress tolerance. *Front. Plant Sci.* **2018**, *9*, 1771. [[CrossRef](#)]
82. Bonaventure, G.; Beisson, F.; Ohlrogge, J.B.; Pollard, M. Analysis of the aliphatic monomer composition of polyesters associated with Arabidopsis epidermis: Occurrence of octadeca-cis-6, cis-9-diene-1,18-dioate as the major component. *Plant J.* **2004**, *40*, 920–930. [[CrossRef](#)]
83. Li-Beisson, Y.; Pollard, M.; Sauveplane, V.; Pinot, F.; Ohlrogge, J.; Beisson, F. Nanoridges that characterize the surface morphology of flowers require the synthesis of cutin polyester. *Proc. Natl. Acad. Sci. USA* **2009**, *106*, 22008–22013. [[CrossRef](#)] [[PubMed](#)]

84. Gupta, N.S.; Collinson, M.E.; Briggs, D.E.; Evershed, R.P.; Pancost, R.D. Reinvestigation of the occurrence of cutan in plants: Implications for the leaf fossil record. *Paleobiology* **2006**, *32*, 432–449. [[CrossRef](#)]
85. Villena, J.F.; Domínguez, E.; Stewart, D.; Heredia, A. Characterization and biosynthesis of non-degradable polymers in plant cuticles. *Planta* **1999**, *208*, 181–187. [[CrossRef](#)] [[PubMed](#)]
86. Göbel, C.; Feussner, I.; Schmidt, A.; Scheel, D.; Sanchez-Serrano, J.; Hamberg, M.; Rosahl, S. Oxylipin profiling reveals the preferential stimulation of the 9-lipoxygenase pathway in elicitor-treated potato cells. *J. Biol. Chem.* **2001**, *276*, 6267–6273. [[CrossRef](#)]
87. Fammartino, A.; Cardinale, F.; Göbel, C.; Mène-Saffrané, L.; Fournier, J.; Feussner, I.; Esquerré-Tugayé, M.T. Characterization of a divinyl ether biosynthetic pathway specifically associated with pathogenesis in tobacco. *Plant Physiol.* **2007**, *143*, 378–388. [[CrossRef](#)]